Research Square

Preprints are preliminary reports that have not undergone peer review.
They should not be considered conclusive, used to inform clinical practice,
or referenced by the media as validated information.

Depositional and Diagenetic Controls on Reservoir Quality in Pre-Salt Carbonates

D. M. Rojas Caro

d227875@dac.unicamp.br

Universidade Estadual de Campinas (UNICAMP)

A. Batezelli

Universidade Estadual de Campinas (UNICAMP)

Research Article

Keywords: Reservoir characterization, mineralogy, structural compartmentalization, carbonate reservoirs, Brazilian Pre-salt

Posted Date: November 11th, 2026

DOI: https://doi.org/10.21203/rs.3.rs-11380977/v1

License: This work is licensed under a Creative Commons Attribution 4.0 International License.
Read Full License

Additional Declarations: No competing interests reported.

Depositional and Diagenetic Controls on Reservoir Quality in Pre-Salt Carbonates

D.M. Rojas Caro[1*,a], A. Batezelli[1,b]

[1]Centro de Estudos de Energia e Petróleo (CEPETRO), Universidade Estadual de Campinas (UNICAMP), Campinas, São Paulo, Brazil

[a]d227875@dac.unicamp.br

[b]batezeli@unicamp.br

Abstract

Reservoir quality in the Barra Velha Formation is controlled by the interaction between depositional facies, diagenetic processes, and mineralogical composition, resulting in marked vertical and lateral petrophysical heterogeneity. This study evaluates these controls in the production intervals of Barra Velha Formation on the Tupi Field, Santos Basin, Brazil. Flow units (FUs) were defined from effective porosity and horizontal permeability using the Flow Zone Indicator (FZI) and cumulative S-curve approach, and subsequently integrated with sedimentological, mineralogical, well-log, and seismic data. Four FUs were identified, ranging from low-quality FU1 ($\log(FZI) < -0.1$) to highly connected FU4 ($\log(FZI) > 0.7$). FU4 is predominantly associated with reworked, calcite-rich shrubstone facies and contains >80% calcite, whereas FU1 shows greater mineralogical variability, including dolomite, quartz, and stevensite-bearing intervals. Stevensite-rich intervals are characterized by restricted permeability and an anomalous elastic response, with relatively low acoustic impedance despite poor reservoir quality. The distribution of FUs also varies markedly among reservoir intervals: BVE100 is dominated by FU2 (57%), BVE200 by FU1 (73%), whereas BVE300 contains mainly FU2 (48%) and FU1 (40%). These relationships were propagated away from well control through probabilistic pre-stack geostatistical seismic inversion. One hundred stochastic realizations were generated for each reservoir interval, and validation at wells excluded from the inversion showed differences of less than 10% between observed and simulated FU proportions. Effective porosity was co-simulated from elastic properties and FU distributions, whereas horizontal permeability was modeled from FU-dependent porosity–permeability relationships because of its weak correlation with seismic elastic properties. The results show that reservoir quality in the Barra Velha carbonates is primarily controlled by depositional and diagenetic heterogeneity and that mineralogical effects, particularly stevensite occurrence, can decouple elastic response from hydraulic quality. Accounting for these controls is therefore required to predict the three-dimensional distribution of reservoir quality beyond well control.

Keywords: Reservoir characterization; mineralogy; structural compartmentalization; carbonate reservoirs; Brazilian Pre-salt

Introduction

Brazilian pre-salt carbonate reservoirs are characterized by marked petrophysical heterogeneity resulting from the interaction of depositional processes and wide diagenetic modification (Lima et al., 2019; Azevedo et al., 2021; Cataldo et al., 2022). Cementation by calcite, dolomite and silica, dolomitization, selective dissolution, recrystallization, micritization and precipitation of Mg-rich clay minerals such as stevensite can substantially modify primary pore systems and connectivity (Carvalho et al., 2022; Schrank et al., 2024). Consequently, porosity alone may not adequately describe reservoir quality or fluid-flow behaviour in these rocks (Corbett, 2015; Matonti et al., 2021).

The Barra Velha Formation is a representative example of this complexity. Its lacustrine depositional system comprises carbonate facies affected by multiple diagenetic processes and later structural compartmentalization, producing strong vertical and lateral variations in reservoir properties (Wright and Barnett, 2015; Gomes et al., 2020; Barbosa et al., 2025). In the Tupi Field, it is subdivided into the three production intervals (BVE100, BVE200 and BVE300; Buckley et al., 2015; Minzoni et al., 2019; Rebelo et al., 2022; Rojas et al., 2023). These intervals show contrasting petrophysical characteristics related to differences in sedimentary facies and diagenetic

alteration (Mattos et al., 2022; Rebelo et al., 2022; Yang et al., 2025). Understanding how these geological controls explain into changes in reservoir quality is therefore important for representing the internal heterogeneity of the Barra Velha Formation.

Lithofacies and porosity are commonly used to describe reservoir heterogeneity, but their relationship with hydraulic behaviour is not necessarily straightforward in diagenetically modified carbonates. Diagenetic process (dolomitization, silicification, dissolution, stevensite precipitation, etc.) can modify pore connectivity and elastic properties without preserving a simple relationship with depositional facies or bulk porosity (Herlinger et al., 2017; Carvalho et al., 2022; Hazaveie et al., 2024; Li et al., 2020). This is particularly relevant in lacustrine carbonates, where similar depositional products may develop contrasting petrophysical responses after different diagenetic histories. Reservoir-quality assessment therefore requires the hydraulic response of the rock to be considered together with its depositional and mineralogical attributes.

Flow-unit (FU) classification provides a means of grouping rocks according to their hydraulic behaviour. Among the available approaches, the Flow Zone Indicator (FZI) relates effective porosity and permeability through the Reservoir Quality Index and has been applied to distinguish flow domains in heterogeneous carbonate reservoirs (Rebelo et al., 2022). Combined with cumulative S-curve analysis, FZI can identify changes in hydraulic behaviour that are not readily represented by lithofacies or porosity alone (Penna, 2022; Penna and Lupinacci, 2024). However, hydraulic classification does not by itself establish the depositional and diagenetic processes responsible for these contrasts. Linking FUs to facies and mineralogical composition is therefore necessary to determine whether changes in reservoir quality reflect depositional organization, diagenetic overprint, or the combined effect of both.

A further challenge is the propagation of these relationships away from well control. Core, plug and well-log data resolve reservoir heterogeneity at centimetre-to-metre scales, whereas conventional seismic data have a vertical resolution of approximately 20–30 m in the study interval. As a result, thin barriers, baffles and high-permeability zones may remain unresolved by deterministic seismic interpretation (Faleide et al., 2021; Rebelo et al., 2022; Vital et al., 2022; Penna and Lupinacci, 2024). Geostatistical seismic inversion provides a means of integrating well-scale geological and petrophysical information with seismic data while retaining multiple realizations of the spatial distribution of reservoir properties (Soares, 2001; Fernandes et al., 2024; Penna and Lupinacci, 2024). This approach is particularly relevant where reservoir quality is controlled by geological features occurring below conventional seismic resolution.

This study investigates the depositional and diagenetic controls on reservoir quality in the production intervals of the Barra Velha Formation in the Tupi Field. FUs are defined from effective porosity and horizontal permeability using FZI and cumulative S-curve analysis and are integrated with sedimentological facies and mineralogical data to evaluate the geological controls on hydraulic behaviour. The elastic response of the resulting FUs is then used in probabilistic pre-stack geostatistical seismic inversion to assess their three-dimensional distribution beyond well control. Effective porosity and horizontal permeability models are subsequently constrained by the flow-unit framework. The study therefore addresses two related questions: (1) how depositional and diagenetic processes control reservoir-quality contrasts in the Barra Velha carbonates, and (2) to what extent these contrasts can be propagated from well to reservoir scale using their elastic response.

Study area

The Santos Basin is Brazil's largest offshore sedimentary basin and its main hydrocarbon province. Located in southeastern Brazil (Figure 1A), it extends between latitudes 23° and 28° S and covers approximately 350,000 km². It is bounded by the Campos and Pelotas basins and flanked by the São Paulo Plateau to the east and the Serra do Mar range to the west (Macedo, 1989; Moreira et al., 2007; Gamboa et al., 2008). The basin developed following the fragmentation of Gondwana (~140 Ma) and the subsequent opening of the South Atlantic Ocean during the Neocomian (Szatmari, 2000). Its tectonostratigraphic evolution records the main stages of passive-

margin development, including lithospheric extension, basement reactivation, crustal breakup, and thermal subsidence (Chang et al., 1992; Cainelli and Mohriak, 1999; Zalán et al., 2009; Petersohn, 2013; Mohriak et al., 2021).

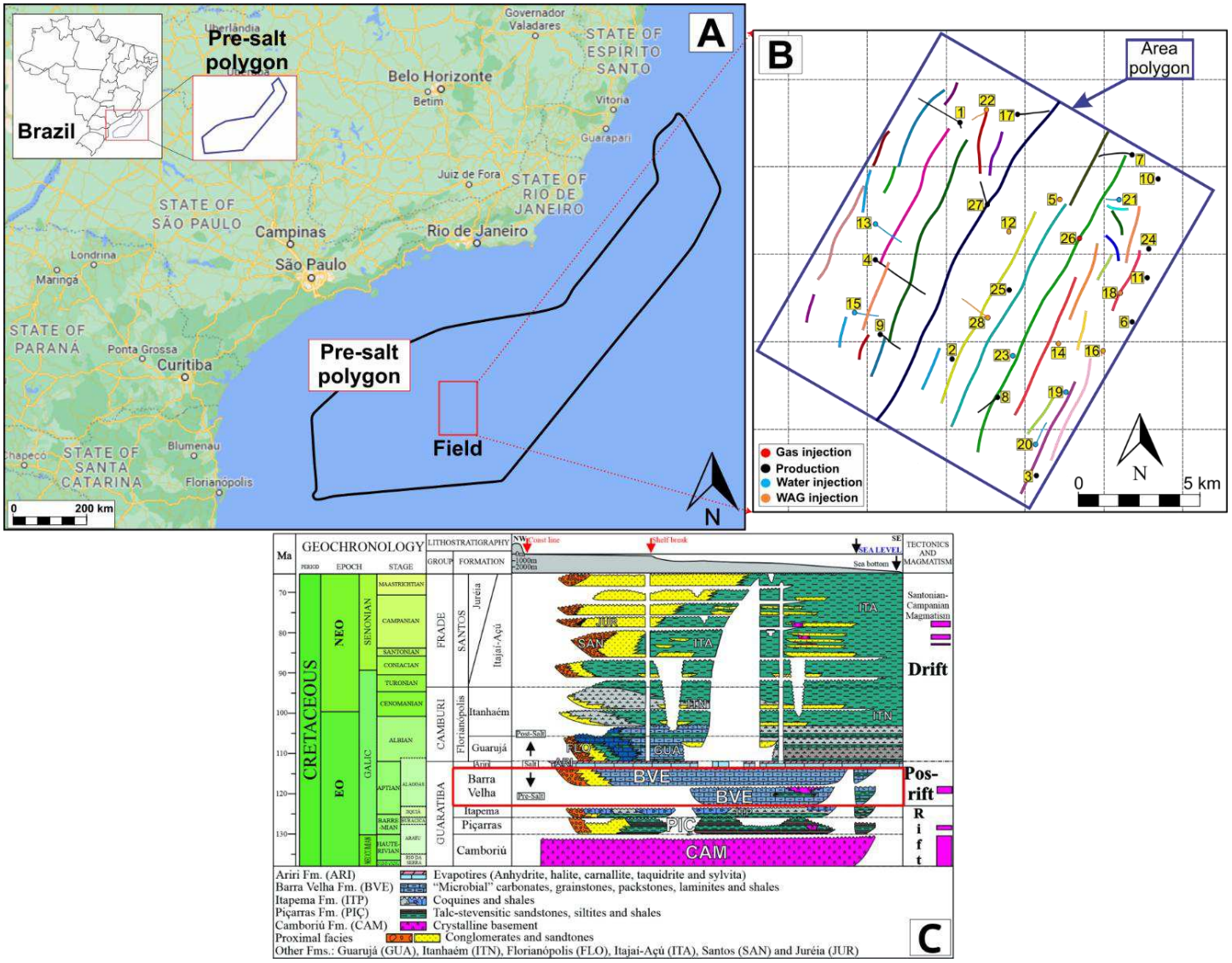


Fig. 1 – Location of the study area: A. study area and the pre-salt polygons; B. wells used in the study (14 selected wells out of 28 wells in the area) (modified from Rojas (2022) and Rojas et al. (2023)); and C. tectonostratigraphic chart of the Cretaceous period of the Santos Basin (modified from Moreira et al., 2007; Rojas et al., 2023).

The sedimentary succession comprises three major supersequences associated with distinct tectonostratigraphic stages (Figure 1C): Rift (Camboriú, Piçarras, and Itapema formations), Post-Rift/Sag (Barra Velha Formation), and Drift (Ariri and post-salt formations) (Pereira and Feijó, 1994; Mohriak, 2003, 2012, 2021; Moreira et al., 2007). The Ariri Formation represents the main evaporitic unit and forms the regional seal above the pre-salt succession (Mohriak, 2001). The Barra Velha Formation represents the Post-Rift/Sag succession at the top of the pre-salt section. Deposited mainly during the Aptian, it comprises microbial carbonates, stromatolites, and mudstones in proximal settings, whereas shale-rich successions predominate distally. Upper Aptian deposits overlie the Lower Aptian succession across an unconformity and include proximal alluvial-fan sandstones and conglomerates and distal microbial carbonates interbedded with shales (Chang et al., 1992; Moreira et al., 2007; Carminatti et al., 2009; Terra et al., 2010; Mann and Rigg, 2012). The Barra Velha carbonates are predominantly abiotic and developed in highly alkaline lacustrine environments (Wright and Barnett, 2015).

The study area corresponds to the OBN Pilot Area of the Tupi Field, in the central Santos Basin (Figure 1A and 1B). The petroleum system comprises lacustrine source rocks of the Piçarras Formation and carbonate reservoirs of the Barra Velha and Itapema formations, regionally sealed by the Ariri evaporites (Chang et al., 2008). The area was selected for intensive reservoir development and geophysical monitoring using Ocean Bottom Nodes (OBN). Production began in 2009 with well 3-BRSA-496-RJS. The study area includes 14 wells, comprising seven producers and seven injectors, including five water injectors, two WAG wells, and one gas injector (Rosa et al., 2018; Cruz et al., 2021).

Material and methods

This study integrates well, core, petrophysical, sedimentological, and seismic data from the BVE100, BVE200, and BVE300 reservoir intervals of the Barra Velha Formation. The well dataset comprises 14 wells distributed across the study area (Figure 1B). Available data include: (a) well trajectories and stratigraphic tops; (b) conventional well logs; (c) nuclear magnetic resonance (NMR) logs and derived petrophysical properties (NMRT, NMREff, NMRff, and NMRK); (d) core-derived porosity and permeability measurements; (e) thin-section data and sedimentological interpretations from Rebelo et al. (2022); and (f) check-shot and vertical seismic profile (VSP) data for well-to-seismic calibration. Where Vs measurements were unavailable, Vs was estimated using multivariate regression following Rojas (2023). After log conditioning, compressional (Zp) and shear (Zs) impedances were calculated.

The seismic dataset was acquired using Ocean Bottom Nodes (OBN) in 2015 and covers approximately 344 km² (Supplementary Figure S1). The acquisition comprised 956 nodes distributed along 36 receiver lines with 50 × 50 m spacing (Cypriano et al., 2019; Cruz et al., 2021). Seismic processing included water-layer deconvolution, ghost-wavefield attenuation, zero-phasing, Kirchhoff Pre-Stack Depth Migration (PSDM), and velocity-model building. The pre-stack data were separated into five partial-angle stacks: Near (0°–13°), Near-Mid (10°–20°), Mid (18°–28°), Far (25°–35°), and Ultra-Far (33°–40°). The seismic data have a dominant frequency of approximately 12 Hz, with the amplitude spectrum shown in Figure 3. Post-stack seismic volumes were used for horizon interpretation and fault mapping and provided the structural framework adopted in this study (Rojas et al., 2023), following the processing workflows described by Cabrera and Rojas (2019) and Illidge et al. (2021). The five pre-stack angle volumes were subsequently used for geostatistical seismic inversion to generate stochastic realizations of Zp, Zs, and density (ρ).

The methodological workflow was organized into four main stages (Figure 2): (1) definition of hydraulic flow units from porosity and permeability data; (2) evaluation of depositional and mineralogical controls on the identified flow units; (3) assessment of their elastic response and probabilistic propagation through geostatistical seismic inversion; and (4) modeling of effective porosity and permeability-related properties conditioned by the flow-unit framework.

[1] Flow-unit definition

Flow units (FUs) were defined from effective porosity (ϕe) and horizontal permeability (Ki) measured in core samples and supplemented by NMR-derived petrophysical properties. The classification followed the Flow Zone Indicator (FZI) approach and cumulative S-curve analysis proposed by Penna and Lupinacci (2020, 2021, 2024). Reservoir Quality Index (RQI) and FZI were calculated as:

$$\mathbf{RQI} = \mathbf{0.0314}\sqrt{\frac{\mathbf{K}}{\mathbf{\Phi_e}}} \quad \text{(Eq. 3)}$$

$$\mathbf{FZI} = \frac{\mathbf{RQI}}{\mathbf{\Phi_z}} \quad \text{(Eq. 4)}$$

where k is horizontal permeability (mD), ϕe is effective porosity expressed as a fraction, and ϕz is the normalized porosity term:

$$\Phi_z = \frac{\Phi_e}{1-\Phi_e} \quad \text{(Eq. 5)}$$

$$\log(\mathrm{RQI}) = \log(\mathrm{FZI}) + \log(\Phi_z) \quad \text{(Eq. 6)}$$

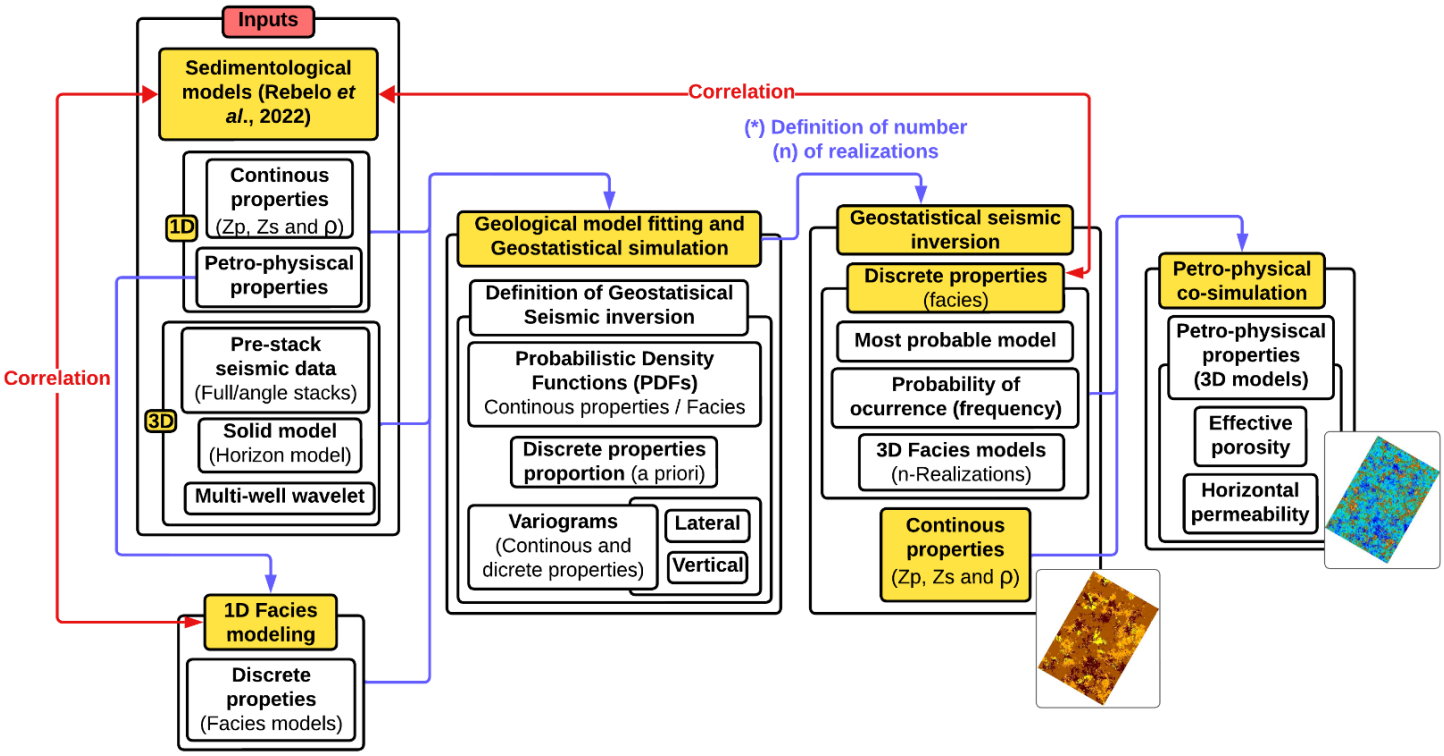


Fig. 2 – Workflow for 3D modelling of FUs and petrophysical properties correlated with sedimentological facies in Brazilian Pre-Salt Carbonates.

The FU boundaries were determined from the cumulative S-curve following Penna and Lupinacci (2024). Effective porosity and permeability data were first ranked and converted to percentiles, from which RQI and FZI were calculated. The data were then ordered by log(FZI), and cumulative normalized permeability was plotted against log(FZI). Changes in the slope of this relationship were used to identify transitions between hydraulic domains. Steep segments indicate intervals with a greater contribution to flow capacity and higher connectivity, whereas low-gradient segments represent lower-connectivity or low-transmissivity domains. The main inflection points were used as thresholds for FU discretisation.

The resulting FU classification was propagated to the well-log scale using NMR-derived effective porosity and permeability, providing continuous FU profiles across the BVE100, BVE200, and BVE300 intervals. These profiles were subsequently compared with sedimentological and mineralogical data to investigate the geological controls on the observed hydraulic behaviour.

[2] Depositional and mineralogical controls on flow units

The sedimentological framework adopted in this study follows Rebelo et al. (2022) and integrates well logs, more than 4,000 routine core analysis (RCA) measurements of porosity and permeability, and petrographic descriptions of more than 400 thin sections under plane- and cross-polarized light. Lithofacies were classified according to Gomes et al. (2020), who defined 12 carbonate facies subsequently grouped according to their sedimentological characteristics and degree of reworking.

The FU profiles defined from FZI and cumulative S-curve analysis were compared with this sedimentological framework to evaluate the depositional controls on hydraulic behaviour. For each reservoir interval (BVE100, BVE200, and BVE300), FU occurrence was analysed in relation to lithofacies, sedimentological associations, depositional setting, and degree of sediment reworking. This comparison was used to determine whether differences in hydraulic behaviour were systematically associated with depositional architecture or represented petrophysical variability within individual facies.

Mineralogical data were subsequently integrated with the FU classification to evaluate the diagenetic overprint on reservoir quality. Mineral composition derived from X-ray diffraction (XRD) and available spectroscopic logs was compared among FUs, with particular attention to variations in calcite, dolomite, quartz, and stevensite occurrence. These data were used to assess whether mineralogical changes could explain variations in porosity, permeability, and elastic response that were not accounted for by depositional facies alone.

[3] **Elastic response and geostatistical seismic inversion**

The elastic response of the flow units was evaluated prior to geostatistical seismic inversion to determine whether differences in hydraulic behaviour were associated with distinguishable elastic properties. Crossplots were generated independently for the BVE100, BVE200, and BVE300 intervals using well-derived elastic properties. Lamé parameters were calculated from compressional velocity (Vp), shear velocity (Vs), and bulk density (ρ) as:

$$\lambda = \rho(V_p^2 - 2V_s^2) \quad \text{(Eq. 7)}$$

$$\mu = \rho V_s^2 \quad \text{(Eq. 8)}$$

where λ and μ are the first and second Lamé parameters, respectively, ρ is bulk density, and Vp and Vs are compressional- and shear-wave velocities. The distribution and overlap of FUs in the elastic domain were examined to assess their seismic separability before inversion.

Probabilistic pre-stack geostatistical seismic inversion was subsequently applied to propagate the FU framework and elastic properties beyond well control. The inversion followed a Bayesian formulation based on the Metropolis–Hastings Markov chain Monte Carlo (MCMC) algorithm, integrating the five partial-angle seismic stacks with well-derived elastic properties and prior FU distributions (Soares, 2001; Soares et al., 2007, 2011; Saussus and Sams, 2012; Kneller et al., 2019; Penna and Lupinacci, 2024). Spatial continuity was represented by variogram models, whereas probability density functions (PDFs) described the statistical distributions of Zp, Zs, density (ρ), and their relationships with the FUs.

The inversion was performed independently for BVE100, BVE200, and BVE300 to preserve the specific FU proportions and elastic-property distributions of each reservoir interval. Starting from prior geological and statistical distributions, the Metropolis–Hastings algorithm iteratively perturbed the model properties. For each proposed realization, elastic properties were converted to synthetic seismic responses by convolution with the corresponding wavelets and compared with the observed partial-angle seismic data. Model perturbations were accepted or rejected according to their posterior probability, allowing the Markov chain to sample models consistent with both the seismic response and the prior geological information.

One hundred stochastic realizations were generated for each reservoir interval. The ensemble of realizations was used to derive three-dimensional probability distributions of FU occurrence and corresponding Zp, Zs, and ρ volumes. The resulting models therefore represent both the most persistent spatial patterns and the variability among equiprobable reservoir scenarios. Wells excluded from the inversion were used as control data, and observed and simulated FU proportions were compared to evaluate the consistency of the inversion results.

[4] Petrophysical property modelling

Effective porosity (ϕe) was co-simulated using the 3D FU distributions and the elastic properties (Zp, Zs, and ρ) obtained from the geostatistical seismic inversion, following the geostatistical approaches of Deutsch and Journel (1997) and Soares et al. (2007). The relationships between ϕe and the elastic properties were defined separately for each FU and reservoir interval (BVE100, BVE200, and BVE300), allowing the porosity models to preserve the petrophysical variability associated with the hydraulic framework.

Horizontal permeability (Ki) was modelled separately because its direct statistical relationship with Zp, Zs, and ρ was weak. Rather than conditioning Ki directly to the elastic properties, FU-dependent relationships between effective porosity and horizontal permeability were established for each reservoir interval. Permeability was then simulated using ϕe and the corresponding FU as conditioning variables. This procedure preserves the distinct porosity–permeability relationships associated with different hydraulic domains without imposing poorly supported correlations between permeability and seismic elastic properties.

One hundred realizations of the petrophysical properties were generated consistently with the stochastic FU and elastic-property models. The ensemble of realizations was used to represent spatial variability in effective porosity and horizontal permeability and to assess the uncertainty associated with their three-dimensional distribution.

Results

[1] Hydraulic behaviour and flow-unit distribution

The FZI and cumulative S-curve analysis distinguished four hydraulic domains (FU1–FU4) within the BVE100, BVE200, and BVE300 intervals (Figure 3). The main inflection points in the relationship between log(FZI) and cumulative normalized permeability define the boundaries between units with contrasting contributions to flow capacity. FU1 represents the lowest-quality hydraulic domain, with log(FZI) < −0.1, whereas FU4 represents the highest-connectivity domain, with log(FZI) > 0.7 (Table 1). FU2 and FU3 occupy intermediate hydraulic domains between these end members. Low-gradient segments of the cumulative curve are predominantly associated with FU1 and FU2, whereas FU3 and FU4 occur along higher-gradient segments associated with increasing flow capacity.

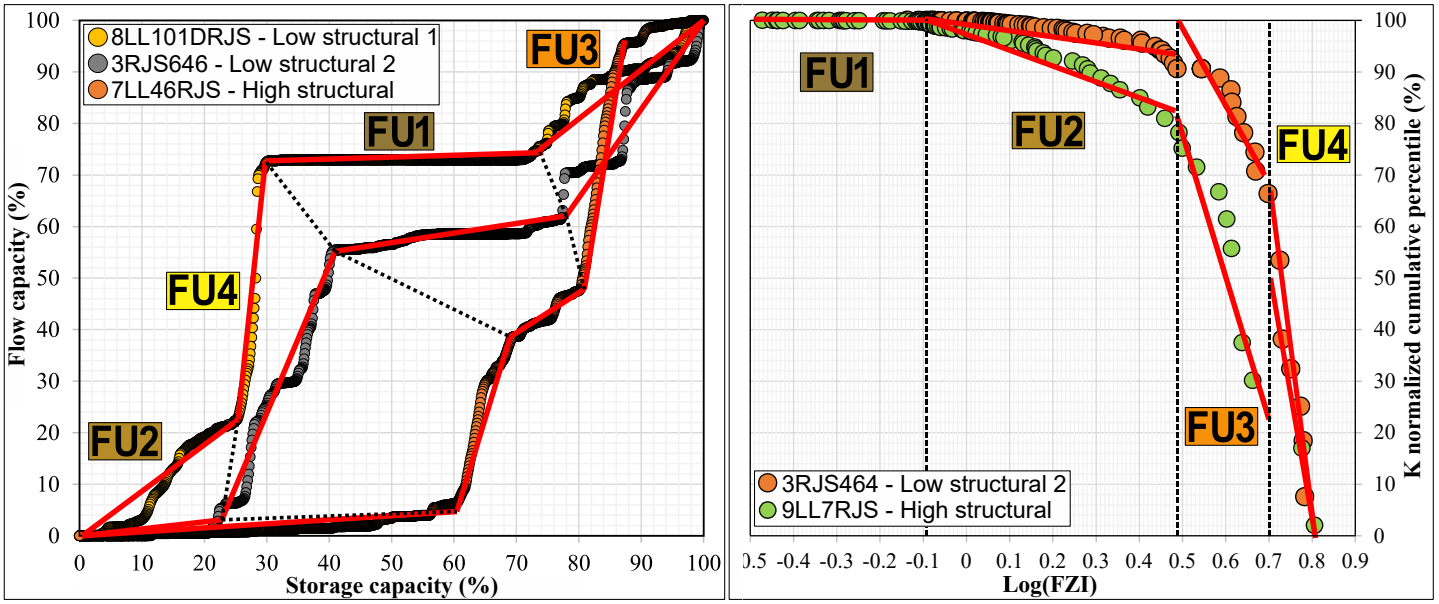


Fig. 3 – Left: Flow capacity curves vs. storage capacity by FU (slope: high connectivity zone; plane: sealing or low transmissivity zone). Right: FUs delimited by Log (FZI) vs. K normalised cumulative percentile (%).

Table 1 – FUs cut-offs from Log (FZI) vs. K normalised cumulative percentile (%) chart

FUs	Log (FZI) values
FU1	Below -0.1
FU2	-0.1 to 0.49
FU3	0.49 to 0.7
FU3	Above to 0.7

The vertical distribution of the four FUs is illustrated in well 9RJS687D (Figure 4). FU3 and FU4 coincide with intervals of higher effective porosity and horizontal permeability, whereas FU1 occurs predominantly in intervals with lower petrophysical quality. The relative occurrence of these units varies among BVE100, BVE200, and BVE300, indicating that the three reservoir intervals contain different proportions and vertical arrangements of hydraulic domains.

Integration of the FU profiles with XRD and spectroscopic data reveals systematic mineralogical differences among the hydraulic domains (Figure 5 and Supplementary Figure S2). FU4 is compositionally more homogeneous and contains >80% calcite, with comparatively low proportions of dolomite and quartz. In contrast, FU1 and FU2 show greater mineralogical variability, including calcite, dolomite, quartz, and stevensite-bearing intervals. FU1 is particularly associated with mineralogically heterogeneous intervals and lower flow quality.

[2] Mineralogical controls on reservoir quality

These compositional differences are accompanied by changes in the relationship between effective porosity and compressional impedance (Zp) (Supplementary Figure S3). The BVE100, BVE200, and BVE300 intervals contain populations that plot within different mineralogical domains defined by the elastic bounds of Hashin and Shtrikman (1963) and Mello and Lupinacci (2022). BVE100 contains a distinct high-Zp population associated with dolomitic compositions, whereas BVE300 shows a broader dispersion of both elastic and petrophysical properties. BVE200 is dominated by the low-quality FU1 domain and contains a greater contribution from clay-rich intervals. Stevensite-bearing carbonates show a distinct response in the effective-porosity–Zp domain. These samples occur predominantly toward lower Zp values but do not exhibit a corresponding increase in effective porosity. Consequently, low compressional impedance does not consistently indicate improved reservoir quality in stevensite-bearing intervals. This effect is observed across the three reservoir intervals and is most evident within the lower-quality FUs.

[3] Depositional controls on reservoir quality

The distribution of FUs varies systematically among the BVE100, BVE200, and BVE300 intervals and their corresponding depositional associations (Figures 6 and 7). The paleoenvironmental model of Rebelo et al. (2022) defines a transition from deeper lacustrine settings to shoreface, foreshore, and backshore environments based on petrographic descriptions, well logs, and sedimentological associations. This framework was used to compare FU occurrence with depositional setting and the relative proportions of in-situ and reworked facies.

BVE100 is dominated by FU2 (57%), followed by FU1 (23%), FU3 (15%), and FU4 (5%). Upper and lower foreshore deposits account for 50.8% and 23.2% of the interval, respectively. In-situ (52.8%) and reworked facies (46.5%) occur in similar proportions, consistent with the predominance of intermediate hydraulic quality and the local occurrence of higher-connectivity domains. BVE200 shows a contrasting relationship between depositional setting and hydraulic behaviour. FU1 accounts for 73% of the interval despite the predominance of upper (47.7%) and lower (39.4%) foreshore deposits. In-situ facies represent 72.8% of the sedimentological association, whereas reworked deposits are subordinate.

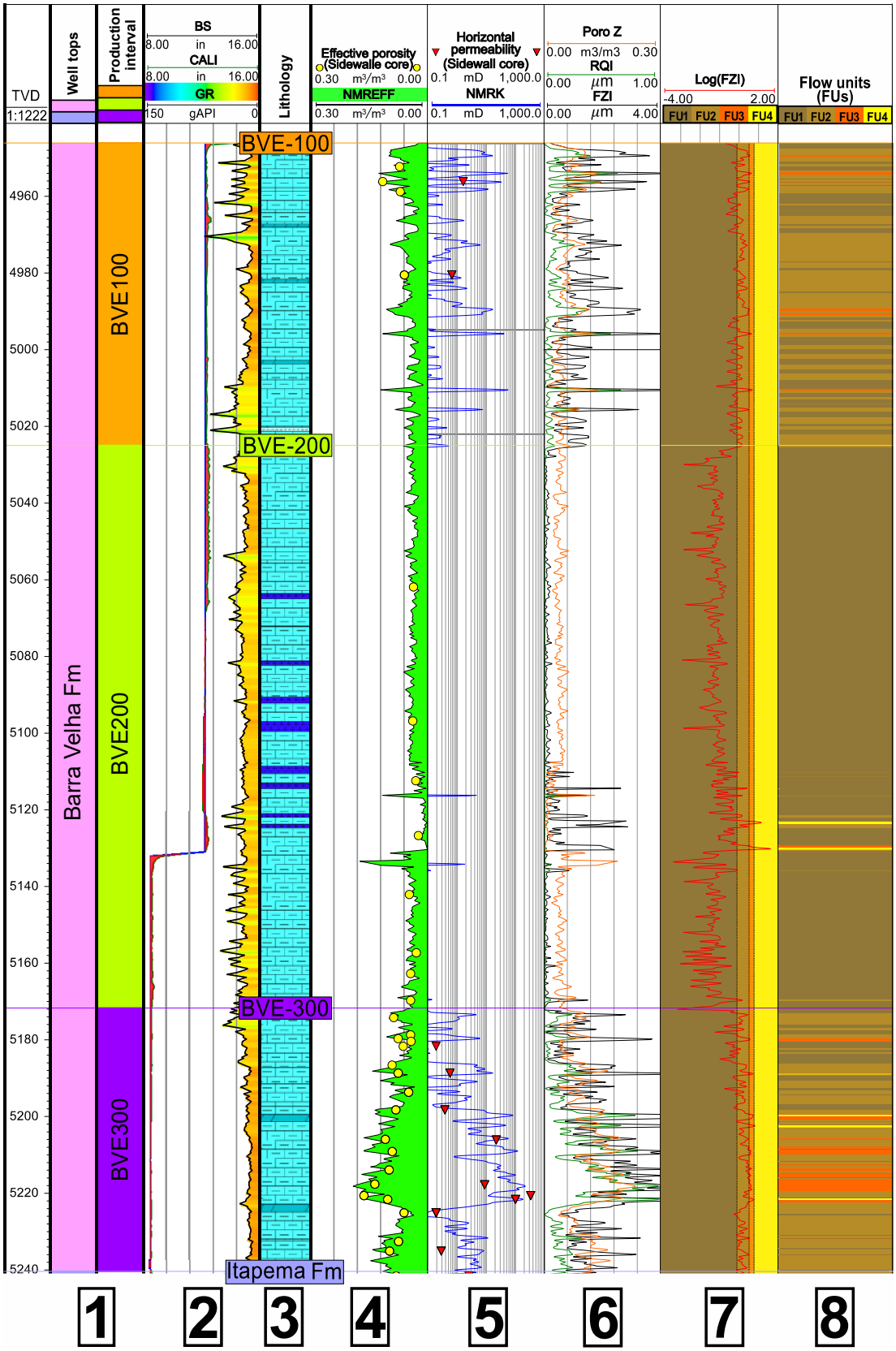


Fig. 4 – Flow units (FUs) models for the production intervals (BVE100, BVE200 e BVE300) of Barra Velha Formation in the well 9RJS687D: (1) Barra Velha Formation and production intervals; (2) bit-size (BS), caliper (CALI) and gamma-ray (GR); (3) lithology; (4) effective porosity (NMREFF and core data); (5) horizontal permeability (NMRK and core data); parameter for the definition of FUs models: (6) Φz, Reservoir Quality Index (RQI) and Flow Zone Indicator (FZI) and (7) log (FZI); and (8) FUs model.

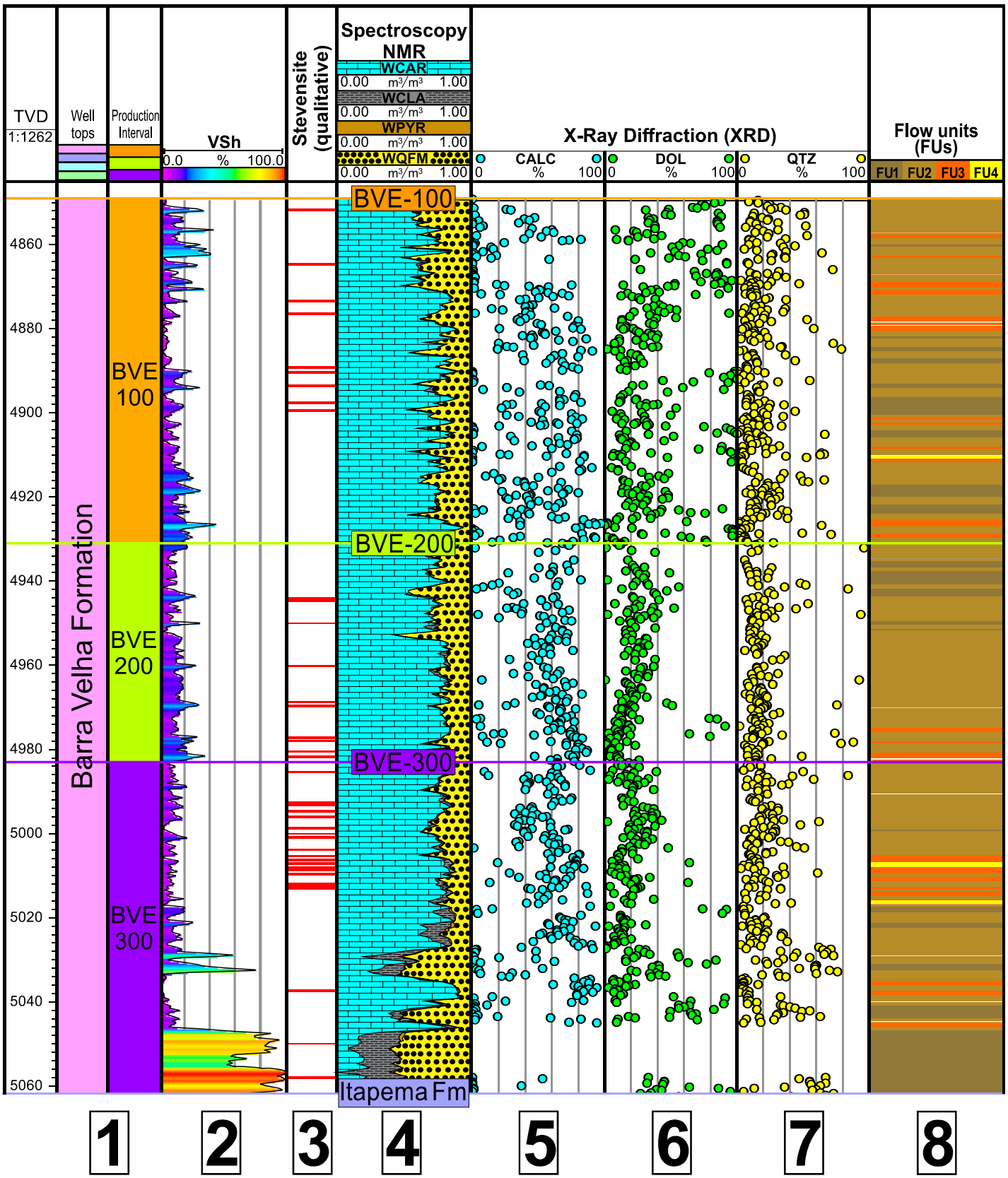


Fig. 5 – Flow units (FUs) models and X-Ray Diffraction (XRD) for the production intervals (BVE100, BVE200 e BVE300) of Barra Velha Formation in the well 9RJS687D: (1) Barra Velha Formation and production intervals; (2) VSh model; (3) stevensite occurrences (qualitative); (4) spectroscopy (NMR) logs: WCAR – carbonates, WCLA – claystone, WPYR – pyrite and WQFM – siliciclastic (quartz, feldspar and mica); X-Ray Diffraction (XRD) : (5) calcite – CALC, (6) dolomite (DOL) and (7) quartz (QTZ); and (8) FUs model.

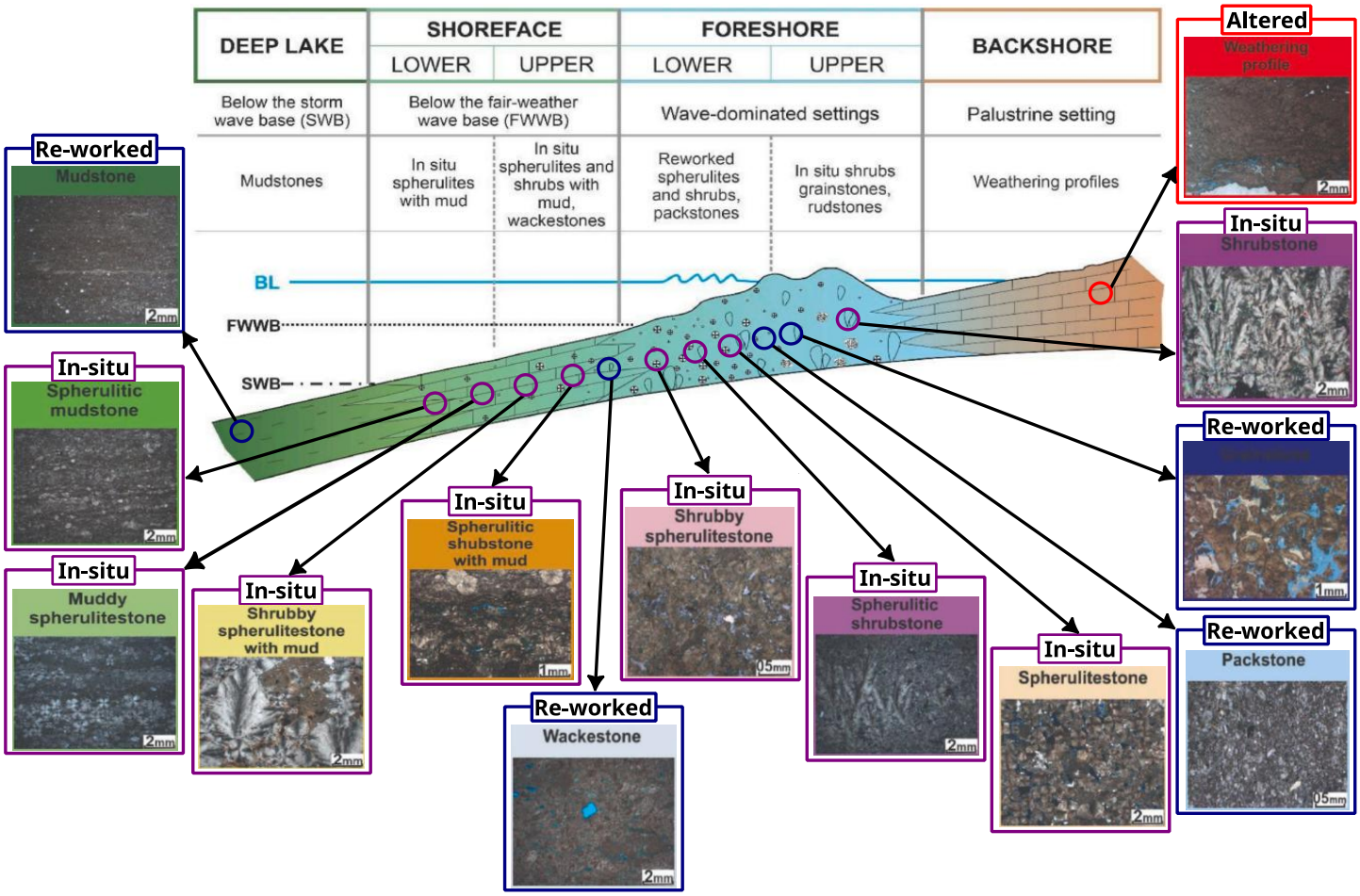


Fig. 6 – Model of the distribution of sedimentological facies of the Barra Formation, distributed in four zones: Deep Lake, Shoreface (lower and upper), Foreshore (lower and upper), and Backshore (modified from Tucker and Wright, 1990 and Rebelo et al., 2022). Sedimentological classification (thin sections of in situ facies: Shrubstone, Spherulitestone, Spherulitic shrubstone, Shrubby spherulitestone, Spherulitic shrubstone with mud, Shrubby spherulitestone with mud, Muddy spherulitestone and Spherulitic mudstone; reworked: Grainstone, Wackestone and Mudstone; and weathering profile - Gomes et al., 2020) of the Barra Velha Formation, proposed by Rebelo et al. (2022). Light base (LB), FWWB (fair weather wave base (FWWB)), SWB (storm wave base (SWB)).

Thus, the predominance of a relatively high-energy depositional setting does not correspond to improved hydraulic quality in BVE200. BVE300 contains 48% FU2 and 40% FU1, with FU3 and FU4 occurring locally. Upper foreshore deposits represent 58.8% of the interval, while reworked facies account for 66% of the sedimentological association. Compared with BVE200, the greater contribution of reworked deposits is associated with a more heterogeneous FU distribution and a larger contribution from higher-connectivity hydraulic domains.

[4] Elastic expression of reservoir-quality domains

The hydraulic domains show partially distinct elastic responses in the λρ–μρ space (Figure 8). FU1 is preferentially distributed toward higher λρ and μρ values, whereas FU4 occupies predominantly lower values. FU2 and FU3 show intermediate distributions and substantial overlap with the two end-member hydraulic domains. The degree of separation varies among BVE100, BVE200, and BVE300, indicating that the elastic expression of reservoir quality is interval dependent. The probability distributions of Zp, Zs, and density (ρ) further illustrate the elastic variability associated with the four FUs (Supplementary Figure S4). Although considerable

overlap occurs between adjacent hydraulic domains, particularly FU1–FU2 and FU2–FU3, the end-member FUs show contrasting elastic-property distributions. These differences provide statistical information for conditioning the probabilistic inversion, while the observed overlap indicates that FU occurrence cannot be uniquely inferred from individual elastic properties.

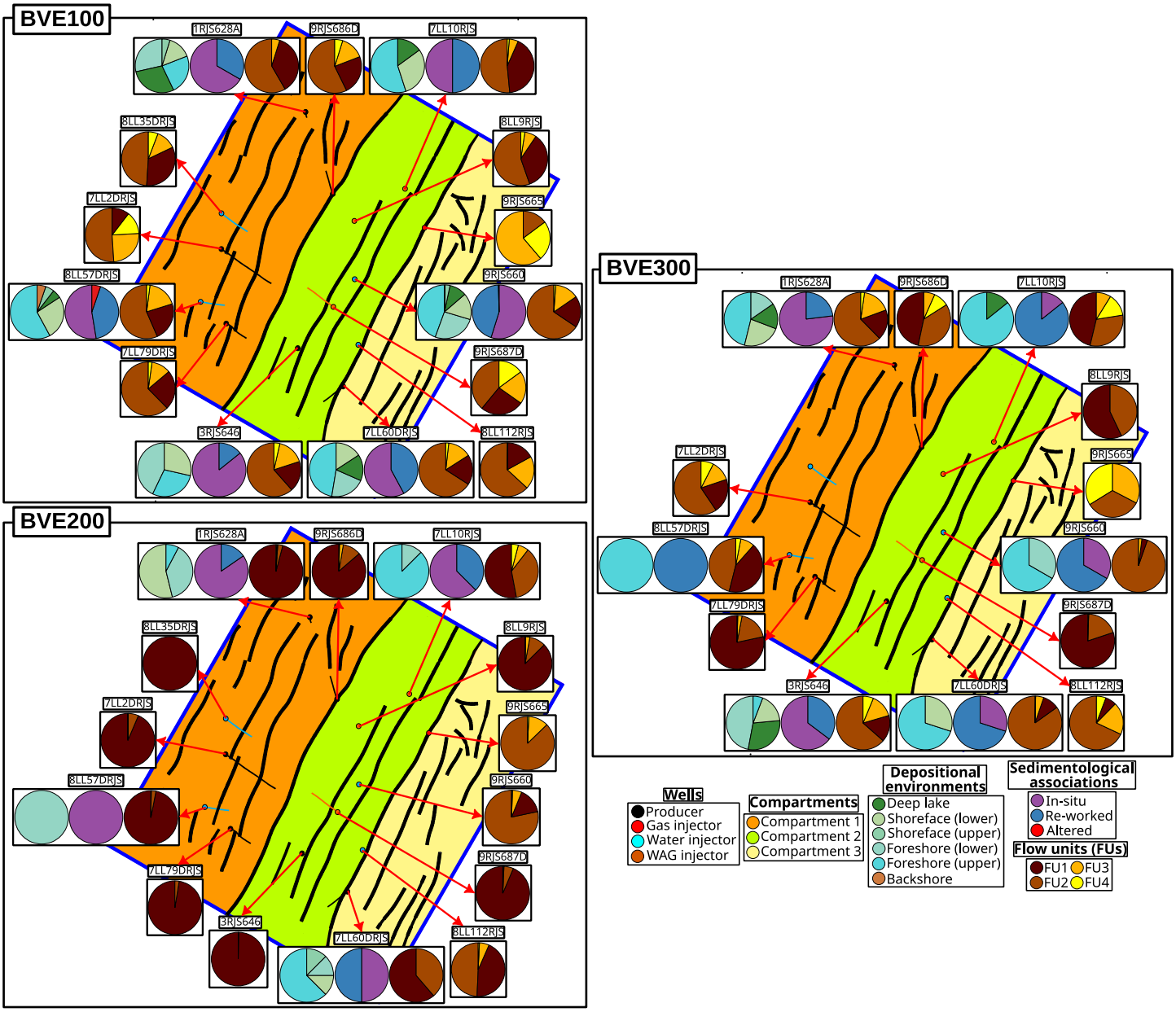


Fig. 7 – Distribution of depositional environments, sedimentological associations, and FUs and their relationship with the structural compartmentalisation of the production intervals (BVE100, BVE200, and BVE300) of the Barra Velha Formation in the study area.

[5] Probabilistic 3D distribution of reservoir-quality domains

The prior FU proportions differ substantially among the three reservoir intervals (Supplementary Figure S5), reflecting the hydraulic contrasts identified from the well data. These interval-specific proportions, together with the FU-dependent elastic-property distributions, were incorporated into independent geostatistical inversions for BVE100, BVE200, and BVE300. Validation against wells excluded from the inversion shows that the simulated FU proportions reproduce the observed distributions with differences below 10%

(Supplementary Figure S6). The agreement is observed across the three reservoir intervals, indicating that the main FU proportions are preserved away from the conditioning wells.

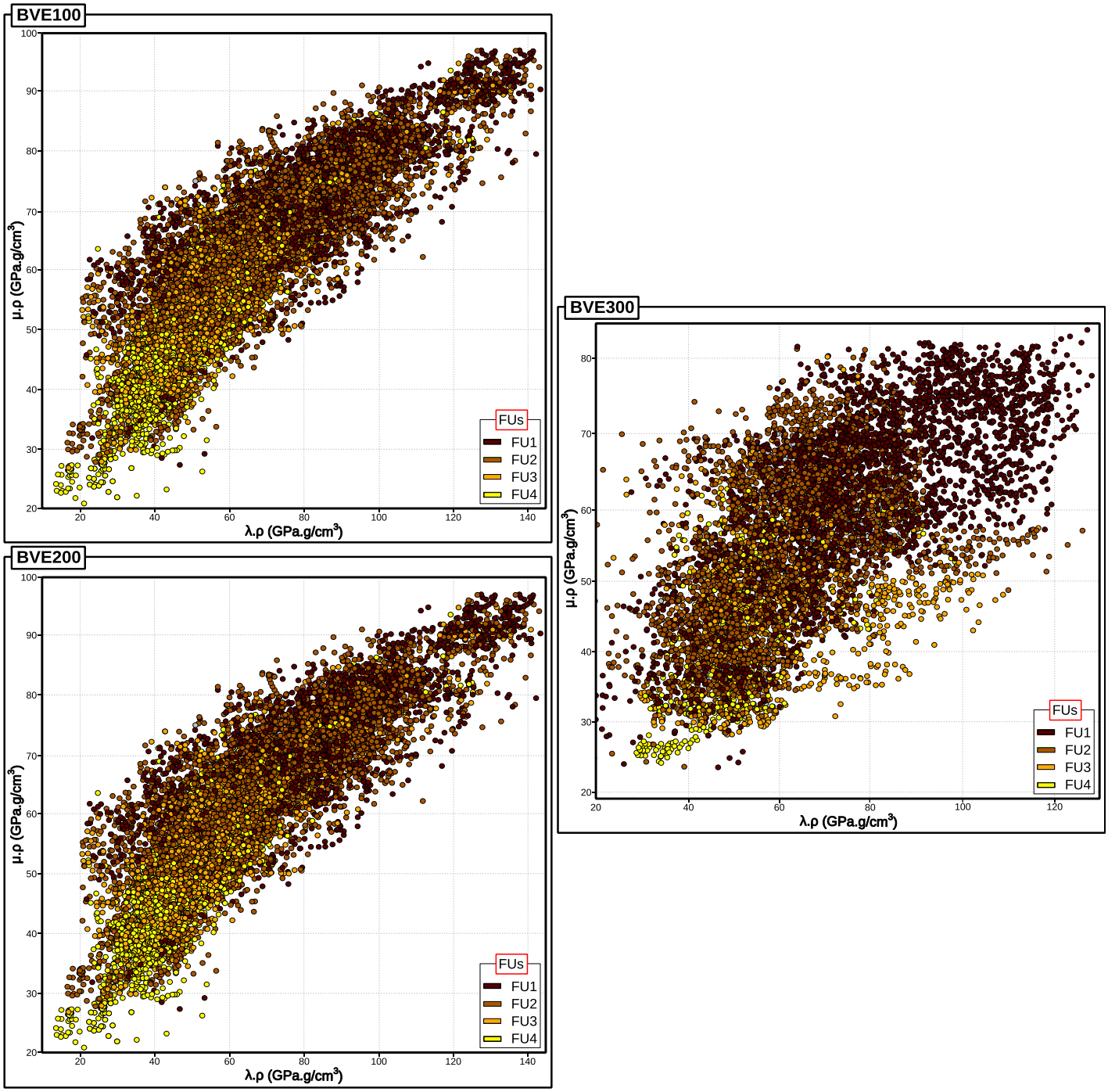


Fig. 8 – Relation to elastic properties (λρ × μρ) for assessing the feasibility of seismic inversion limited by FUs for the production intervals (BVE100, BVE200, and BVE300) of the Barra Velha Formation.

The 100 stochastic realizations generated for each interval were used to calculate the probability of occurrence of each FU (Figure 9). BVE100 is characterized by a high probability of FU2 over much of the interval, particularly in the structurally higher areas. In BVE200, FU1 has the highest probability and shows broad lateral continuity, whereas FU2 occurs locally. BVE300 exhibits a more heterogeneous probability distribution, with FU1 and FU2 occurring in comparable proportions and FU3 becoming locally significant. FU4 has a consistently low probability of occurrence.

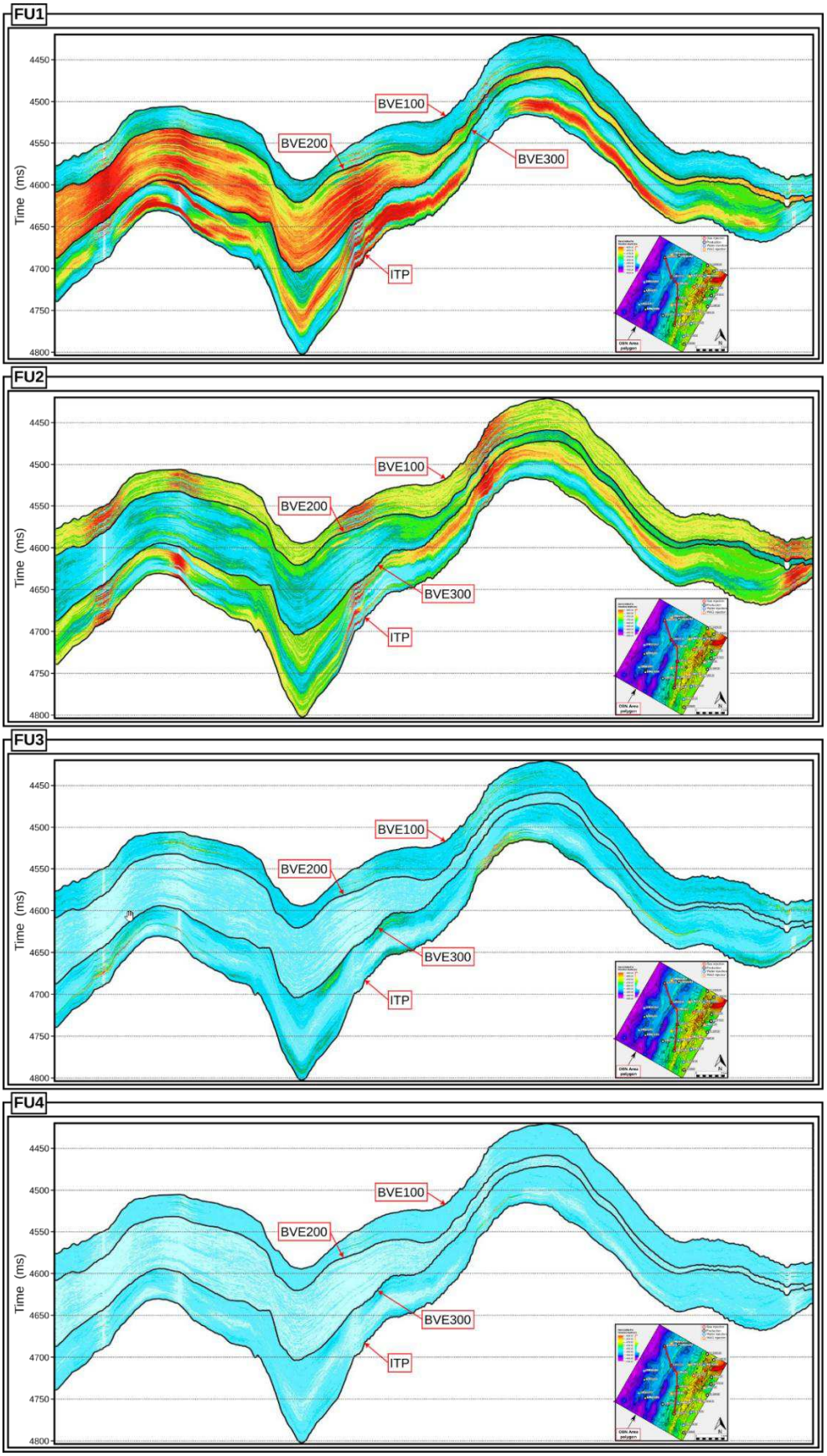


Fig. 9 – N–S cross section showing the probability of occurrence of the displayed flow-unit classes across the BVE100, BVE200, and BVE300 intervals of the Barra Velha Formation, along a representative section intersecting five wells. Probabilities were derived from 100 stochastic realizations. FU4, which has a low overall occurrence, is discussed in the text; its visualization in this figure should be checked against the original panels.

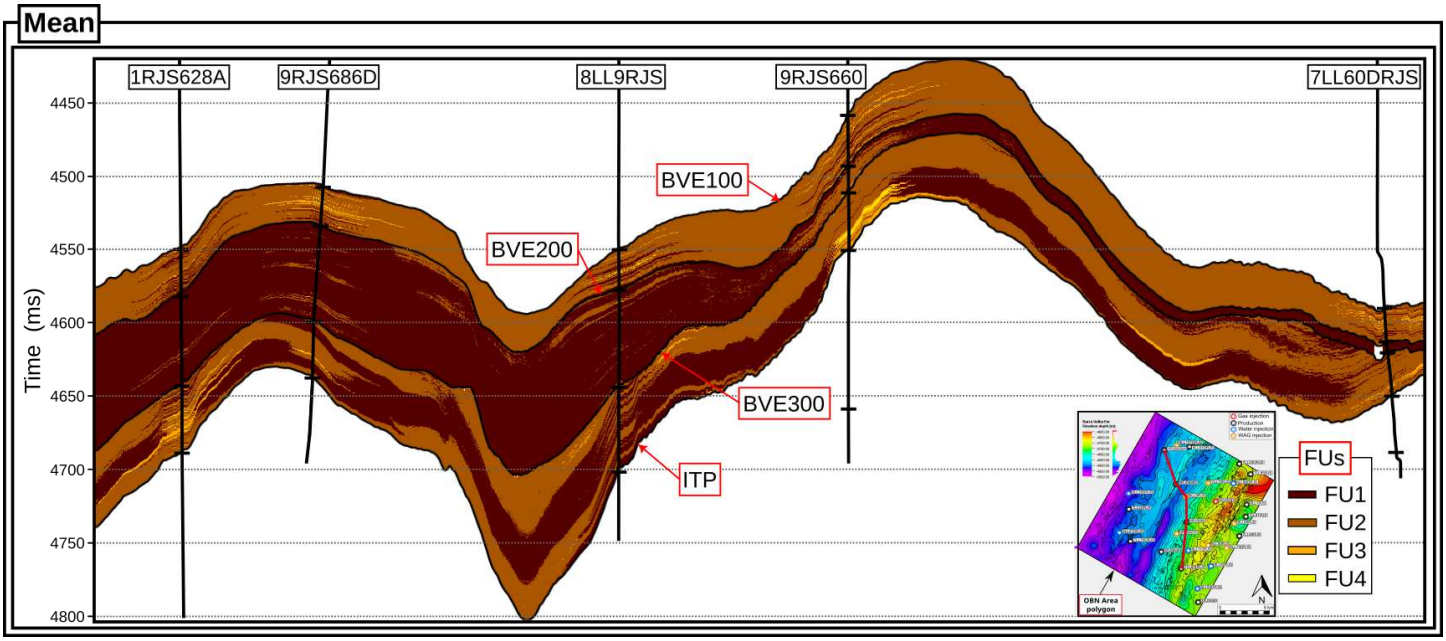


Fig. 10 – N–S cross section of the ensemble-derived flow-unit model for the BVE100, BVE200, and BVE300 intervals of the Barra Velha Formation, calculated from 100 stochastic realizations along a representative section intersecting five wells.

The ensemble-derived model summarizes the spatial distribution of FUs across the 100 realizations (Figure 10). It highlights first-order differences among reservoir intervals, with FU2 prevailing in BVE100, FU1 in BVE200, and a mixed FU1–FU2 distribution in BVE300. Individual stochastic realizations may retain additional local variability, but are not shown here.

[6] Petrophysical architecture and spatial variability

Effective porosity (ϕe) was modelled using the stochastic FU distributions and elastic properties obtained from the geostatistical seismic inversion. The ensemble-mean effective-porosity model shows marked differences among the three reservoir intervals (Figure 12). BVE100 is characterized by intermediate to high ϕe, with laterally continuous higher-porosity zones occurring predominantly within FU2. BVE200 shows the lowest ϕe values and the most spatially homogeneous distribution, consistent with the predominance of FU1. In contrast, BVE300 exhibits greater lateral and vertical variability, with localized higher-porosity zones associated mainly with FU3 and FU4.

The NMR-derived permeability index (Ki) shows a different relationship with the conditioning variables. Direct relationships between Ki and the elastic properties Zp, Zs, and ρ were weak; therefore, permeability was not directly conditioned to the seismic-derived elastic properties. Instead, class-dependent relationships between effective porosity and the NMR-derived permeability index were established separately for each reservoir interval (Figure 11). These relationships show that similar effective-porosity values can correspond to different permeability ranges depending on the associated hydraulic domain.

The resulting Ki models indicate contrasting permeability architectures among the three reservoir intervals (Fig. 12). BVE100 is characterized predominantly by moderate permeability associated with FU2, with relatively continuous lateral patterns interrupted by lower-permeability FU1 domains. BVE200 has the lowest and most spatially homogeneous permeability distribution, consistent with the predominance of FU1 and its lower effective porosity. BVE300 exhibits the greatest lateral and vertical permeability variability, with higher-Ki zones associated locally with FU3 and FU4 and lower-permeability regions corresponding predominantly to FU1.

Comparison of the ϕe and Ki models indicates that porosity alone does not fully reproduce the spatial variability in hydraulic quality.

This is particularly evident where comparable porosity values occur within different FUs but correspond to different permeability ranges. The FU-conditioned petrophysical models therefore preserve the distinct porosity–permeability relationships identified among the hydraulic domains.

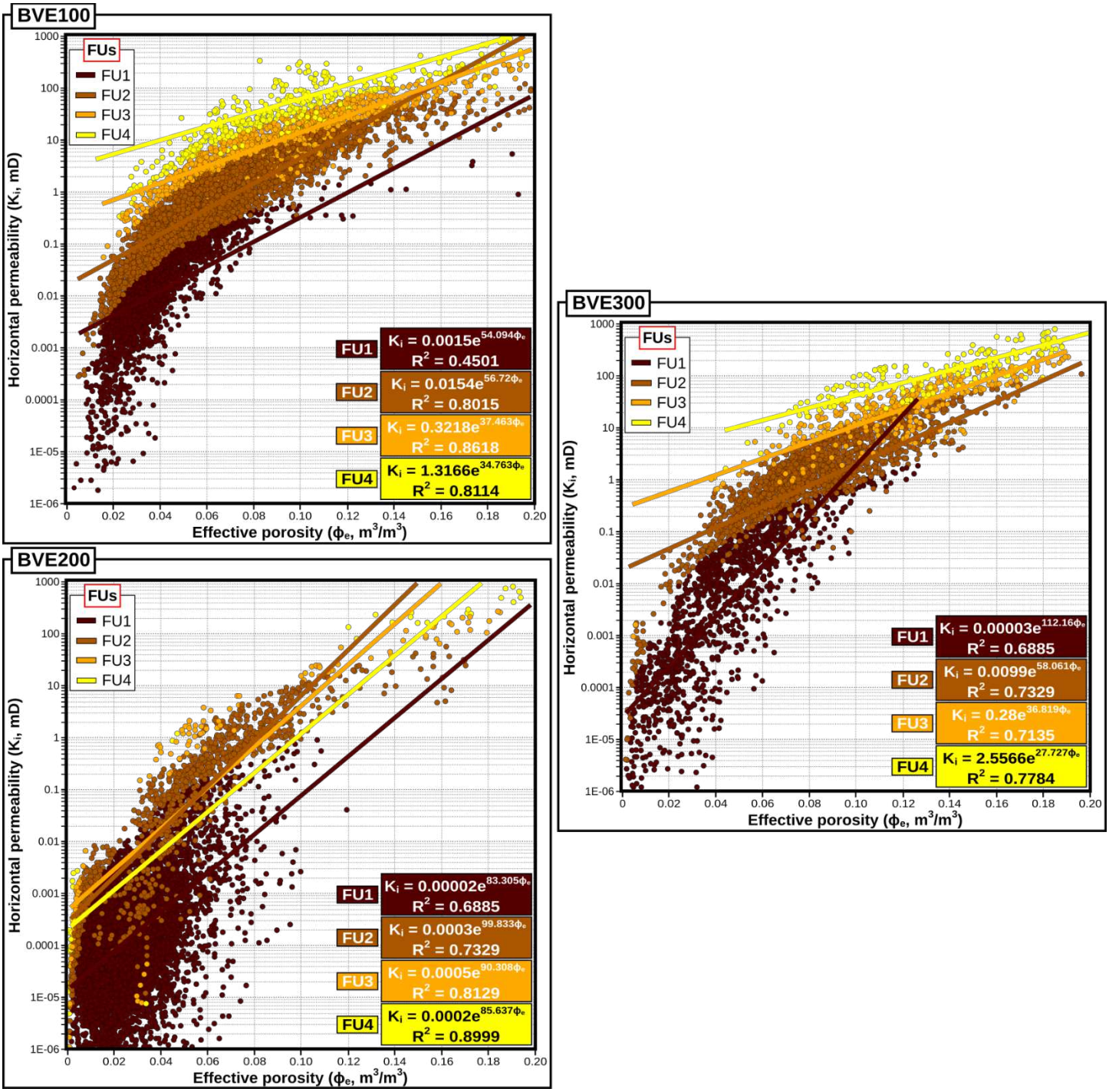


Fig. 11 – Crossplots of effective porosity (ϕe) versus NMR-derived permeability index (Ki) for the BVE100, BVE200, and BVE300 intervals of the Barra Velha Formation, classified by hydraulic flow units (FUs). Lines show FU-specific regression trends; annotations report fitted coefficients and coefficients of determination (R^2).

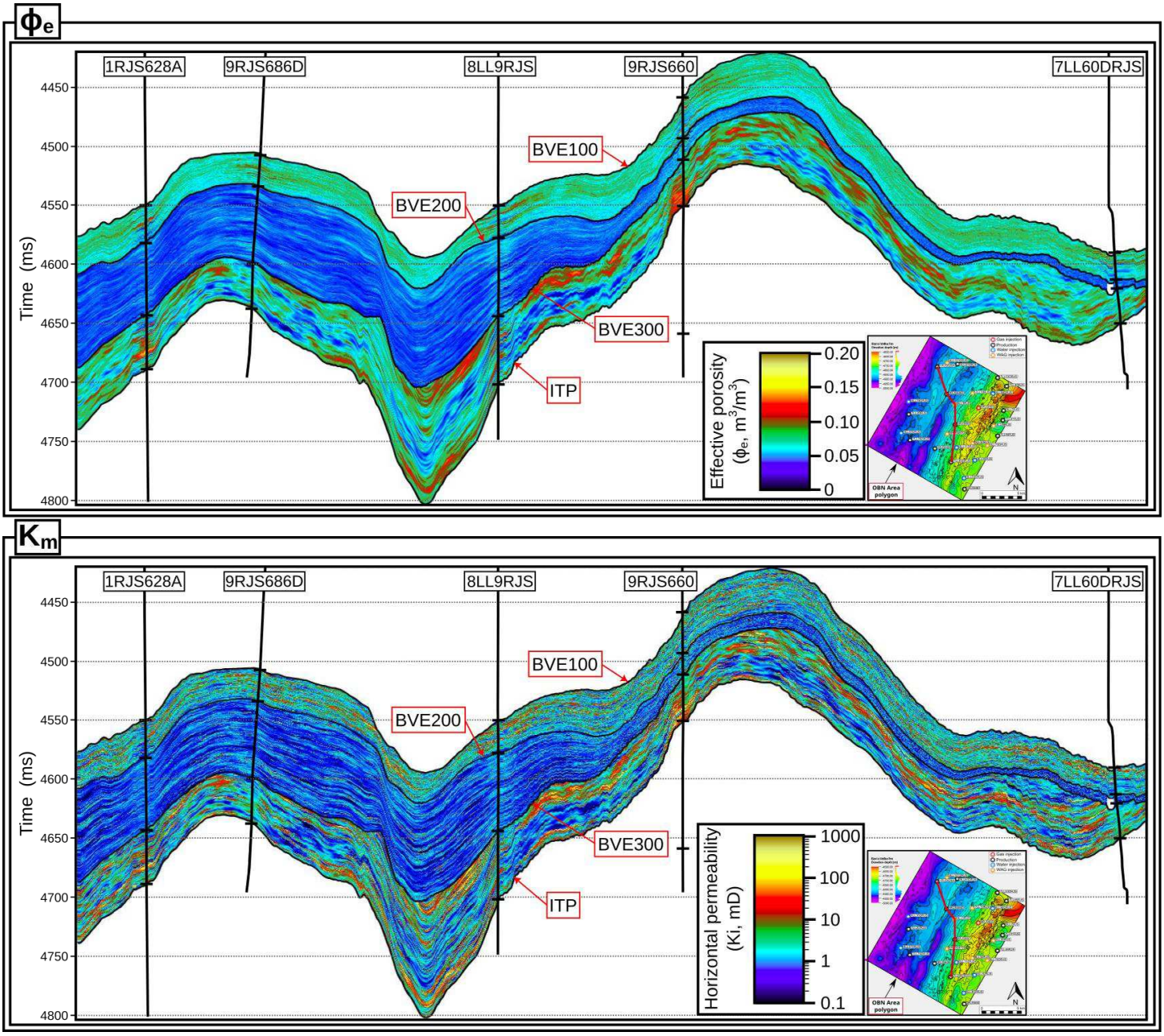


Fig. 12 – N-S cross section of the ϕe and Ki models for the production intervals (BVE100, BVE200 and BVE300) of the Barra Velha Formation: mean (average of 100 realizations). Section crossing along a representative N–S section crossing five wells.

Discussion

[1] Depositional and diagenetic controls on reservoir quality

The relationship between depositional facies and FUs indicates that depositional processes establish an important first-order control on reservoir quality in the Barra Velha Formation, but do not uniquely determine hydraulic behaviour. Higher-quality hydraulic domains (FU3 and FU4) occur preferentially in reworked and higher-energy depositional settings, whereas FU1 is more commonly associated with in-situ and mud-rich deposits. This relationship is consistent with the expected effect of sediment reworking on texture and pore connectivity: removal of fine material and redistribution of carbonate grains can favour more open pore systems, whereas preservation of fine-grained matrices tends to restrict connectivity. However, the substantial overlap between sedimentological associations and FUs demonstrates that depositional facies alone cannot predict reservoir quality.

The contrast among BVE100, BVE200, and BVE300 illustrates this relationship particularly well. BVE100 contains similar proportions of in-situ and reworked facies and is dominated by the intermediate-quality FU2, corresponding to effective porosities of approximately 0.12–0.16 and permeability locally exceeding 200 mD. BVE300 contains a larger proportion of reworked facies and exhibits the greatest petrophysical heterogeneity, including local FU3–FU4 domains where effective porosity exceeds 0.18 and horizontal permeability can exceed 800 mD. BVE200, however, provides an important counterexample to a simple depositional-energy control. Despite the predominance of upper and lower foreshore deposits, the interval contains 72.8% in-situ facies and 73% FU1, with effective porosity commonly below 0.08 and horizontal permeability below 50 mD. Thus, depositional setting alone does not account for the observed differences in hydraulic behaviour among the three intervals.

Mineralogical variability provides an additional control on these relationships. FU4 is predominantly calcitic (>80% calcite), whereas the lower-quality FUs show greater compositional variability involving calcite, dolomite, quartz, and stevensite. This association indicates that the hydraulic response preserved within individual depositional domains was subsequently modified by mineralogical and diagenetic processes. Similar sedimentological facies can therefore exhibit different porosity–permeability relationships, while different facies may converge toward similar hydraulic behaviour after diagenetic modification. Comparable decoupling between depositional facies and petrophysical quality has been reported in heterogeneous carbonate reservoirs, where dissolution, cementation, recrystallisation, dolomitization, and clay-mineral occurrence can substantially modify primary pore systems (Lima et al., 2020; Carvalho et al., 2022; Marghani et al., 2022).

The stevensite-bearing intervals provide a particularly relevant example of this diagenetic/mineralogical overprint. These intervals exhibit comparatively low Zp without a corresponding increase in effective porosity or hydraulic quality. Consequently, low impedance cannot be interpreted systematically as evidence of improved reservoir quality in the Barra Velha carbonates. The elastic response depends not only on pore volume but also on mineralogical composition and pore-system characteristics. This behaviour helps explain why FU1 can retain poor hydraulic properties while locally displaying an elastic response that would otherwise be associated with more porous rocks.

The FU framework captures this combined depositional and diagenetic control because the classification is based on the relationship between effective porosity and permeability rather than lithological identity alone. The resulting hydraulic domains therefore do not replace sedimentological facies; instead, they provide a complementary description of how depositional textures and subsequent mineralogical modification are expressed in pore connectivity. This distinction is important in the Barra Velha Formation, where lithologically similar intervals may have different permeability at comparable porosity and where individual FUs can occur across more than one sedimentological association (Abdulelah et al., 2018; Oliveira et al., 2020; Rebelo et al., 2022).

The three-dimensional petrophysical models preserve these differences. The relatively continuous intermediate-quality domains in BVE100 contrast with the predominantly low-porosity and low-permeability architecture of BVE200 and the more heterogeneous distribution observed in BVE300. Importantly, the FU-conditioned porosity–permeability relationships show that similar effective porosities can correspond to different permeability ranges depending on the hydraulic domain. This behaviour reinforces the limitation of predicting permeability from porosity or depositional facies alone and supports the use of FUs as an intermediate hydraulic description between geological observations and three-dimensional petrophysical modelling.

[2] Mineralogical control and the role of stevensite

Stevensite represents an important mineralogical control on the relationship between hydraulic quality and elastic response in the Barra Velha carbonates. This Mg-rich smectite, commonly associated with alkaline lacustrine carbonate systems (Furquim et al., 2008;

Buchheim et al., 2014), occurs preferentially within the lower-quality FU1 and FU2 domains and is scarce in FU3 and FU4. Its occurrence is therefore associated with intervals characterized by lower permeability and reduced pore connectivity, consistent with previous observations of Mg-rich clay minerals in pre-salt carbonate pore systems (Herlinger et al., 2017; Lima and Ros, 2019; Carvalho et al., 2022; Silva et al., 2025).

The mineralogical contrasts among FUs extend beyond stevensite occurrence. FU4 contains >80% calcite and comparatively low proportions of dolomite and quartz, whereas FU1 exhibits substantially greater compositional variability, including dolomite-, quartz-, and stevensite-bearing intervals (Supplementary Figure S2). This compositional variability accompanies the broader range of petrophysical and elastic responses observed within FU1. In contrast, the more calcite-dominated composition of FU4 coincides with higher FZI values and the highest-quality hydraulic response. These relationships indicate that hydraulic quality reflects not only depositional texture but also the mineralogical modification of the original pore system (Penna and Lupinacci, 2021; Cataldo et al., 2022; Rebelo et al., 2022).

The influence of mineralogical composition is particularly evident in the relationship between effective porosity and compressional impedance (Supplementary Figure S3). Stevensite-bearing intervals occupy comparatively low-Zp regions without a corresponding increase in effective porosity. FU1 consequently includes intervals characterized by relatively low impedance but poor hydraulic quality, demonstrating that low Zp cannot be interpreted systematically as an indicator of high porosity or improved reservoir quality. This response contrasts with FU4, where lower impedance and density occur together with higher effective porosity and permeability.

The inverted elastic-property models reproduce this non-unique relationship. FU1 locally combines comparatively low Zp and Zs with relatively high density, whereas FU4 generally exhibits lower density and a hydraulic response characterized by higher effective porosity and permeability. The contrasting behaviour indicates that variations in elastic properties cannot be attributed to pore volume alone and must be interpreted together with mineralogical composition, carbonate texture, and diagenetic modification (Dias et al., 2019, 2021; Penna and Lupinacci, 2021; Mello and Lupinacci, 2021; Meireles et al., 2022; Bashir et al., 2024).

Well-log and NMR responses provide independent support for this interpretation. FU1 shows more variable mineralogical signatures and generally lower NMREFF, whereas FU4 is characterized by a more carbonate-dominated composition and higher, more continuous NMREFF values. The agreement among mineralogical data, NMR-derived properties, and FU classification indicates that the anomalous elastic behaviour of the lower-quality domains is associated with differences in both pore-system characteristics and mineralogical composition rather than with effective porosity alone (Al-Dousari et al., 2020; Soares et al., 2023).

These results have an important implication for seismic-scale reservoir-quality prediction. In the Barra Velha Formation, low acoustic impedance may represent either a porous, hydraulically favourable carbonate or a mineralogically distinct interval with poorer hydraulic properties. Stevensite-bearing rocks are particularly relevant to this ambiguity because their elastic response can partially decouple impedance from effective porosity and permeability (Azbel et al., 2016; Oliveira et al., 2016; Dias et al., 2019; Alabbad et al., 2021; Mello and Lupinacci, 2022). Mineralogical and diagenetic information is therefore required to interpret elastic-property variations in terms of reservoir quality, particularly where Mg-rich clay minerals occur.

[3] Structural influence on reservoir-quality distribution

The spatial distribution of reservoir-quality domains also shows a relationship with the structural compartmentalisation of the Barra Velha Formation. Three main compartments bounded by medium- to high-angle normal faults are recognized in the study area, and differences in FU proportions, sedimentological associations, and mineralogical composition occur across these structural domains. Compared with the depositional and diagenetic relationships discussed above, however, the structural framework is interpreted as a

secondary control that modifies the spatial organization and preservation of reservoir heterogeneity rather than directly defining hydraulic quality.

Variations among the structural compartments coincide with changes in the relative abundance of in-situ and reworked deposits and in the distribution of lower- and higher-quality FUs. Domains containing a greater proportion of in-situ and mud-rich deposits are preferentially associated with FU1 and FU2, whereas areas with a greater contribution from reworked deposits contain a larger proportion of FU3 and FU4. Mineralogical variations, including the occurrence of stevensite-bearing intervals, also show spatial differences across the structural framework. These associations suggest that accommodation, depositional reworking, and subsequent diagenetic modification may have interacted with the evolving structural configuration of the reservoir.

Such an interpretation is consistent with studies showing that syn-depositional faulting can influence accommodation, carbonate thickness, and depositional architecture in pre-salt successions (Toledo et al., 2022; Silva et al., 2024). Fault systems may also influence post-depositional fluid circulation and therefore contribute to spatial variations in diagenetic alteration (Netto et al., 2022; Corrêa et al., 2025). In this context, the association observed between structural compartments, mineralogical variability, and FU distribution may reflect both depositional organization and later fluid–rock interaction rather than a direct relationship between fault occurrence and reservoir quality.

The structural framework therefore provides an additional level of organization for the depositional and diagenetic heterogeneity identified in the study area. Its influence is most evident in the spatial arrangement of reservoir-quality domains rather than in a unique FU–fault relationship. This distinction is important because the occurrence of a particular FU cannot be predicted from structural position alone; reservoir quality results from the combined effects of depositional texture, mineralogical and diagenetic modification, and their spatial organization within the faulted reservoir architecture.

[4] Implications for static modelling, simulation, and reservoir development

The integrated methodology proposed, combining hydraulic characterisation via FUs, sedimentological and mineralogical analysis (with emphasis on stevensite), and geostatistical seismic inversion, proved effective in improving the geological fidelity of static models in heterogeneous carbonate systems like the Barra Velha Formation.

Traditionally, pre-salt petrophysical models have limitations: (1) poor correlation between sedimentological and petrophysical facies, limiting lithology- or porosity-based models (Cataldo et al.; 2022; Rodríguez-Berriguete et al.; 2022; Zeitoum et al.; 2024; Matheus et al.; 2025); (2) conventional seismic vertical resolution (20–30 m) fails to capture flow-relevant heterogeneities like baffles or excess-K zones (Teillet et al.; 2020; Cataldo et al.; 2022; Penna and Lupinacci, 2024; Tomassi et al.; 2024); and (3) diagenetic minerals (e.g.; stevensite) are often neglected despite their effect on pore connectivity and elastic response (Carvalho and Fernandes, 2021; Oliveira et al.; 2023; Queiroz et al.; 2024).

Applying FUs as discrete hydraulic units, constrained by well data and propagated through Metropolis-Hastings inversion, helped overcome these limitations. The approach demonstrated that: (1) FU spatial distribution matched well the data, even in unconstrained zones; (2) the elastic separation between FU1 and FU4 was key to capturing real petrophysical contrasts; and (3) the final 3D models preserved geological coherence, depositional continuity, and structural compartmentalisation.

This advance supports models that better represent reservoir connectivity, enabling: (1) optimised well placement; (2) geological interpretation of anomalous production responses; and (3) reduced uncertainty in dynamic simulation by incorporating petrophysical and mineralogical variability. By capturing effects of sedimentary reworking, mud accumulation, and stevensite precipitation, the models are more sensitive to zones with unconventional behaviour—such as low-impedance areas with low productivity.

This work provides a replicable, geologically grounded framework for petrophysical characterization in complex carbonate systems, applicable to the Brazilian pre-salt and to other contexts with lacustrine lithofacies or similar diagenetic evolution.

Conclusion

This study investigated the depositional and diagenetic controls on reservoir quality in the BVE100, BVE200, and BVE300 intervals of the Barra Velha Formation by integrating hydraulic flow units with sedimentological, mineralogical, petrophysical, and seismic data. Four hydraulic domains were identified, ranging from low-quality FU1 ($\log(FZI) < -0.1$) to highly connected FU4 ($\log(FZI) > 0.7$). Their distribution demonstrates that depositional setting provides an important first-order control on reservoir architecture but does not uniquely determine hydraulic quality.

The three reservoir intervals show contrasting relationships between depositional character and hydraulic behaviour. BVE100 is dominated by the intermediate-quality FU2 (57%), whereas BVE200 contains 73% FU1 despite the predominance of upper and lower foreshore deposits. BVE300 is more heterogeneous, with FU2 (48%) and FU1 (40%) dominating and higher-quality FU3–FU4 occurring locally. These contrasts indicate that depositional energy alone cannot explain reservoir quality and that the degree of reworking and subsequent diagenetic modification are important controls on pore connectivity.

Mineralogical composition further modifies these depositional relationships. FU4 is predominantly calcitic (>80% calcite), whereas FU1 is compositionally more heterogeneous and includes dolomite-, quartz-, and stevensite-bearing intervals. Stevensite is particularly important because its occurrence in lower-quality hydraulic domains is associated with comparatively low acoustic impedance without a corresponding increase in effective porosity or permeability. Consequently, low impedance does not uniquely indicate favourable reservoir quality in the Barra Velha Formation, demonstrating that elastic properties must be interpreted together with mineralogical and pore-system characteristics.

The hydraulic domains have partially distinct, but overlapping, elastic signatures. Probabilistic geostatistical inversion therefore provides a more appropriate representation than a deterministic seismic-to-FU relationship. One hundred stochastic realizations for each reservoir interval reproduced the first-order FU architecture, and validation at wells excluded from the inversion showed differences of less than 10% between observed and simulated FU proportions. The resulting models show that effective porosity can be related to the elastic-property and FU distributions, whereas horizontal permeability requires FU-dependent porosity–permeability relationships because of its weak direct correlation with Zp, Zs, and density.

Overall, reservoir quality in the Barra Velha Formation results from the interaction between depositional architecture and subsequent mineralogical and diagenetic modification, with structural compartmentalisation providing an additional spatial control on their distribution. These interactions produce non-unique relationships among facies, porosity, permeability, and elastic properties. Representing this non-uniqueness explicitly is therefore essential when reservoir-quality relationships identified at core and well scale are propagated into three-dimensional models of heterogeneous pre-salt carbonates.

CRediT Author Statement

[1] **Daniel Mauricio Rojas Caro**: Conceptualization, Formal analysis, Investigation, Methodology, Software, Validation, Visualization, Writing – original draft.

[2] **Alessandro Batezelli**: Formal analysis, Funding acquisition, Project administration, Resources, Supervision, Validation, Writing – review & editing.

Declaration of Competing Interests

The authors declare that they have no known competing financial interests or personal relationships that could have appeared to influence the work reported in this paper.

Funding Statement and *Acknowledgements*

The authors thank the Coordination for the Improvement of Higher Education Personnel (CAPES-PROEX) for the financial support and the National Council for Scientific and Technological Development (CNPq) for the productivity grants (processes 310734/2020-7 and 309463/2025-4).

Declaration of Generative AI and AI-assisted technologies in the writing process

During the preparation of this work the author(s) used ChatGPT to check grammar and improve readability. After using this tool, the authors reviewed and edited the content as needed and take full responsibility for the content of the published article.

References

[1] Abdulelah, H.; Mahmood, S. and Hamada, G. (2018). Hydraulic flow units for reservoir characterization: A successful application on Arab-D carbonate. IOP Conference Series: Materials Science and Engineering, 380(1), 012020. https://doi.org/10.1088/1757-899X/380/1/012020

[2] Agar, S. and Geiger, S. (2014). Fundamental controls on fluid flow in carbonates: current workflows to emerging technologies. Geological Society, London, Special Publications, 406, 1–59. https://doi.org/10.1144/SP406.18

[3] Ahr, W. (2008). Geology of Carbonate Reservoirs: The Identification, Description, and Characterization of Hydrocarbon Reservoirs in Carbonate Rocks. John Wiley and Sons, 296 p. ISBN: 978-0-470-13394-3

[4] Alabbad, A.; Dvorkin, J.; Altowairqi, Y.; and Duan, Z. (2021). Rock physics-based interpretation of seismically derived elastic volumes. Frontiers in Earth Science, 8, 620276. https://doi.org/10.3389/feart.2020.620276

[5] Al-Ajmi, F. and Holditch, S. (2000). Permeability estimation using hydraulic flow units in a Central Arabia reservoir. SPE Paper No. 63254. https://doi.org/10.2118/63254-MS

[6] Al-Dousari, M.; Almudhhi, S. and Garrouch, A. (2020). Predicting the flow zone indicator of carbonate reservoirs using NMR echo transforms, and routine open-hole log measurements: Insights from a field case study spanning extreme micro-structure properties. Journal of Engineering Research. https://doi.org/10.36909/jer.13185

[7] Azbel, K.; Rodinha, O.; Baechle, G.; Gouveia, W.; Gracioso, D.; Nogueira, F.; Wang, P. and Centeno, R. (2016). De-risking Reservoir Quality and Presence through Seismic Inversion and Rock Physics Analysis in Brazil's Pre-salt Carbonates. Third EAGE/SBGf Workshop, cp-479-00015. https://doi.org/10.3997/2214-4609.201600057

[8] Azevedo, L. and Soares, A. (2018). Geostatistical methods for reservoir geophysics. Mathematical Geosciences, 50(7), 861–863. https://doi.org/10.1007/s11004-018-9748-8

[9] Barbosa, G.; Garcia, G.; Barberes, G.; Pena, R. and Garcia, A. (2025). Analysis of analogous microbialite reservoirs and their associated petroleum systems in rift and passive margin basins: South Atlantic (Brazil) vs. North Atlantic (Portugal). Frontiers in Earth Science, 13, 1554096. https://doi.org/10.3389/feart.2025.1554096

[10] Barnett, A.; Obermaier, M.; Amthor, J.; Sharafodin, M.; Bolton, M.; Clarke, D. and Camara, R. (2021). Origin and significance of thick carbonate grainstone packages in nonmarine successions: A case study from the Barra Velha Formation, Santos Basin, Brazil. In Memoir 124: The Supergiant Lower Cretaceous Pre-Salt Petroleum Systems of the Santos Basin, Brazil (pp. 155–174). AAPG. https://doi.org/10.1306/13722318MSB.6.1853

[11] Bashir, Y.; Siddiqui, N. and Morib, D (2024). Cohesive approach for determining porosity and P-impedance in carbonate rocks using seismic attributes and inversion analysis. Journal of Petroleum Exploration and Production Technology, 14, 1173–1187. https://doi.org/10.1007/s13202-024-01767-x

[12] Buckley, J.; Bosence, D. and Elders, C. (2015). Tectonic setting and stratigraphic architecture of an Early Cretaceous lacustrine carbonate platform, Sugar Loaf High, Santos Basin, Brazil. Geological Society, London, Special Publication, 418, 1–17.

[13] Cabrera, M. and Rojas, D. (2019). Characterisation petrofísica de yacimientos implementando atributos e inversión sísmica. Trabalho de Conclusão de Curso, Universidade Industrial de Santander.

[14] Cainelli, C. and Mohriak, W. (1999). Some remarks on the evolution of sedimentary basins along the Eastern Brazilian continental margin. Episodes, 22(3), 206–216.

[15] Carminatti, M.; Dias, J. and Wolf, B. (2009). From turbidites to carbonates: Breaking paradigms in deep waters. Offshore Technology Conference, Houston, TX, Paper OTC-20124, 1–13. https://doi.org/10.4043/20124-MS

[16] Carvalho, A.; Hamon, Y.; De Souza Jr, O.; Carramal, N. and Collard, N. (2022). Facies and diagenesis distribution in an Aptian pre-salt carbonate reservoir of the Santos Basin, offshore Brazil: A comprehensive quantitative approach. Marine and Petroleum Geology, 141, 105708. https://doi.org/10.1016/j.marpetgeo.2022.105708

[17] Carvalho, M. and Fernandes, F. L. (2021). Chapter 5: Pre-Salt Depositional System: Sedimentology, Diagenesis, and Reservoir Quality of the Barra Velha Formation, as a Result of the Santos Basin Tectono–Stratigraphic Development. In Memoir 124: The Supergiant Lower Cretaceous Pre-Salt Petroleum Systems of the Santos Basin, Brazil (pp. 121–154). AAPG Datapages. https://doi.org/10.1306/137232337MSB.5.1708

[18] Cataldo, R.; Leite, E.; Rebelo, T. and Mattos, N. (2022). Depth variant pore type modeling in a pre-salt carbonate field offshore Brazil. Frontiers in Earth Science, 10, 1014573. https://doi.org/10.3389/feart.2022.1014573

[19] Chang, H.; Kowsmann, R.; Figueiredo, A. and Bender, A. (1992). Tectonics and stratigraphy of the East Brazil Rift System: An overview. Tectonophysics, 213(1–2), 97–138. https://doi.org/10.1016/0040-1951(92)90252-6

[20] Corbett, P. (2015). Reservoir Characterisation Challenges in Pre-Salt Brazilian Carbonates. Search and Discovery Article #51083. https://www.searchanddiscovery.com/documents/2015/51083corbett/ndx_corbett.pdf

[21] Corrêa, R.; Carvalho, B.; Ukar, E.; Laubach, S.; Pestilho, A.; Fall, A.; Larson, T.; Stockli, D.; Stockli, L.; Lüders, V.; Niedermann, S.; and Banks, D. (2025). Brittle deformation and hydrothermal alteration in the Barra Velha Formation, Santos Basin, offshore Brazil. AAPG Bulletin, 109(4), 545–590. https://doi.org/10.1306/03182524012

[22] Cypriano, L.; Yu, Z.; Ferreira, D.; Huard, B.; Pereira, R.; Jouno, F.; Kialil, A.; Urasaki, E. N. A.; Muniz da Cruz, N.; Yin, A.; Clarke, D. and Cardeal-Jesus, C. (2019). OBN for pre-salt imaging and reservoir monitoring – Potential and road ahead. 16th International Congress of the Brazilian Geophysical Society, Rio de Janeiro, 19–22 August 2019. Sociedade Brasileira de Geofísica (SBGF).

[23] Deutsch, C. and Journel, A. (1997). GSLIB: Geostatistical Software Library and User's Guide (2nd ed.). Oxford University Press, New York.

[24] Dias, R.; Fernandes, F.; Vizeu, F.; Carvalho, T.; Gamboa, L.; Freire, A. and Lupinacci, W. (2021). Understanding the relationship between acoustic impedance and porosity in pre-salt carbonate reservoirs of the Santos Basin using probability density functions (PDF). 17th International Congress of the Brazilian Geophysical Society (SBGf), Rio de Janeiro, Brazil.

[25] Dias, R.; Lupinacci, W.; De Castro, T. and Santos, M. (2019). Understanding the relationship between acoustic impedance and porosity in the presalt of the Buzios Field, Santos Basin. First EAGE Workshop on Pre-Salt Reservoir: from Exploration to Production, Rio de Janeiro. https://doi.org/10.3997/2214-4609.201982009

[26] Doyen, P. (2007). Seismic Reservoir Characterization: An Earth Modelling Perspective (EET 2). EAGE Publications. https://doi.org/10.3997/9789073781771

[27] Faleide, T. S.; Braathen, A.; Lecomte, I.; Mulrooney, M.; Midtkandal, I.; Bugge, A. and Planke, S. (2021). Impacts of seismic resolution on fault interpretation: Insights from seismic modelling. Tectonophysics, 816, 229008. https://doi.org/10.1016/j.tecto.2021.229008

[28] Feng, R.; Luthi, S. M. and Gisolf, D. (2018). Simulating reservoir lithologies by an actively conditioned Markov chain model. Journal of Geophysical Engineering, 15(3), 800–815. https://doi.org/10.1088/1742-2140/aaa0ff

[29] Fernandes, F.; Teixeira, L.; Freire, A. and Lupinacci, W. (2024). Stochastic seismic inversion and Bayesian facies classification applied to porosity modeling and igneous rock identification. Petroleum Science, 21, 918–935. https://doi.org/10.1016/j.petsci.2023.11.030

[30] Ferreira, D. and Lupinacci, W. (2018). An approach for three-dimensional quantitative carbonate reservoir characterization in the Pampo Field, Campos Basin, offshore Brazil. AAPG Bulletin, 102, 2267–2282. https://doi.org/10.1306/04121817352

[31] Figueiredo, I.; Lana, C.; Alkmim, F.; Silva, M. A.; Souza, M. E. S.; Dias-Filho, D. C.; Zambonato, E. E.; and Mendonça, K. R. N. (2025). Tracing carbonate diagenesis and hydrothermal activity during the opening of the Central South Atlantic: Insights from the Santos Basin (Brazil). Geoscience Frontiers, 16(5), 102115. https://doi.org/10.1016/j.gsf.2025.102115

[32] Gamboa, L.; Machado, M.; Silveira, D.; Freitas, J. and Silva, S. (2008). Evaporitos estratificados no Atlântico Sul. Sal: Geologia e Tectônica. Exemplos nas Bacias Brasileiras, Vol. 1, 1–163. Beca Edições, São Paulo.

[33] Gholizadeh, M.; Adabia, M. H.; Sadeghi, A.; Ghasemi, M. and Moradi, M. (2022). Sedimentary Environment, Diagenesis, Sequence Stratigraphy, and Reservoir Quality of the Ilam Formation in Dezful Embayment and Abadan Plain in South-West Iran. arXiv preprint, arXiv:2210.05930. https://doi.org/10.48550/arXiv.2210.05930

[34] Gomes, J.; Bunevich, R.; Tedeschi, L.; Tucker, M. and Whitaker, F. (2020). Facies classification and patterns of lacustrine carbonate deposition of the Barra Velha Formation, Santos Basin, Brazilian Pre-salt. Marine and Petroleum Geology, 113, 104176. https://doi.org/10.1016/j.marpetgeo.2019.104176

[35] Hajibolouri, E.; RooZshenas, A. A.; Miri, R.; Soleymanzadeh, A.; Kord, S.; and Shafiei, A. (2024). Permeability modelling in a highly heterogeneous tight carbonate reservoir using comparative evaluating learning-based and fitting-based approaches. Scientific Reports, 14, 10209. https://doi.org/10.1038/s41598-024-60995-7

[36] Hashin, Z.; and Shtrikman, S. (1963). A variational approach to the theory of the elastic behaviour of multiphase materials. Journal of the Mechanics and Physics of Solids, 11(2), 127–140. https://doi.org/10.1016/0022-5096(63)90060-7

[37] Hazaveie, S.; Aminshahidy, B. and Nikbin, M. (2024). A review of the intrinsic parameters affecting the elastic characteristics of heterogeneous carbonate reservoirs: Insights from laboratory assessments. International Journal of Petroleum Technology, 11, 40–55. https://doi.org/10.15377/2409-787X.2024.11.4

[38] Herlinger, R.; Zambonato, E. and De Ros, L. (2017). Influence of diagenesis on the quality of Lower Cretaceous pre-salt lacustrine carbonate reservoirs from northern Campos Basin, offshore Brazil. Journal of Sedimentary Research, 87, 1285–1313. https://doi.org/10.2110/jsr.2017.70

[39] Homaie, M.; Mahboubi, A.; Hartmann, D. J.; KadKiodaie, A. and Moussavi-Harami, R. (2024) Flow Unit Classification and Characterization with Emphasis on the Clustering Methods: A Case Study in a Highly Heterogeneous Carbonate Reservoir, Eastern Margin of Dezful Embayment, Springer International Publishing: SW Iran, 14. DOI: 10.1007/s13202-024-01847-y

[40] Horta, A. and Soares, A. (2010). Direct sequential co-simulation with joint probability distributions. Mathematical Geosciences, 42(3), 269–292. https://doi.org/10.1007/s11004-010-9265-x

[41] Illidge, E.; Camargo, J. and Pinto, J. (2021). 3D seismic stratigraphy applied to lithology estimation in a deltaic system. Boletín de Geología, 43(2). https://doi.org/10.18273/revbol.v43n2-2021008

[42] KadKiodaie-IlKichi, A. and KadKiodaie-IlKichi, R. (2019). A review of reservoir rock typing methods in carbonate reservoirs: Relation between geological, seismic, and reservoir rock types. Journal of Oil, Gas and Petrochemical Sciences, 2019. https://doi.org/10.22050/jogst.2019.136243.1461

[43] Kialid, M.; Mansour, A.; Desouky, S.; Afify, W.; Ahmed, S. and Elnaggar, O. (2024). Carbonate reservoir characterization and permeability modeling using Machine Learning — a study from Ras Fanar field, Gulf of Suez, Egypt. Earth Science Informatics, 17, 4675–4694. https://doi.org/10.1007/s12145-024-01251-2

[44] Kneller, E.; Teixeira, L.; Hak, B.; Cruz, N.; Oliveira, T.; Cruz, J. and Cunha, R. (2019). Challenges and solutions of geostatistical inversion for reservoir characterization of the Supergiant Lula Field. Petroleum Geostatistics, 1–5. https://doi.org/10.3997/2214-4609.201902176

[45] Leite, M.; Amancio Novo, T. and Reis, H. (2024). Exploring the Tupi Field: Insights into Structural Controls on Diagenesis in Brazil's Largest Oil Reserve. Joint 120th Annual Cordilleran / 74th Annual Rocky Mountain Section Meeting, Geological Society of America. Abstracts with Programs, Vol. 56, No. 4.

[46] Leite, M.; Novo, T.; Reis, H.; Fonte-Boa, T.; Moura-Costa, F.; and Costa, D. (2025). Interplay between Structural Framework and Diagenetic Processes in the Barra Velha Formation: A Study from Tupi Field, Santos Basin, Brazil. SSRN. https://ssrn.com/abstract=4820715

[47] Leite, M.; Welch, M. and Fabricius, I. (2022). Relation of acoustic impedance to stiffness and porosity of Maastrichtian chalk in Dan field, Danish North Sea. Geophysical Prospecting, 70(7), 1228–1242. https://doi.org/10.1111/1365-2478.13218

[48] Li, Q.; You, X.; Jiang, Z.; Wu, S. and Zhang, R. (2020). The origins of carbonate minerals of a source-controlled lacustrine carbonate succession in the Shulu sag, Bohai Bay Basin: Implications for porosity development and paleoenvironment. Marine and Petroleum Geology, 122, 104673. https://doi.org/10.1016/j.marpetgeo.2020.104673

[49] Lima, B. and De Ros, L. (2019). Deposition, diagenetic and hydrothermal processes in the Aptian Pre-Salt lacustrine carbonate reservoirs of the northern Campos Basin, offshore Brazil. Sedimentary Geology, 383, 55–81. https://doi.org/10.1016/j.sedgeo.2019.01.006

[50] Lima, M. C. O.; Pontedeiro, E. M.; Ramirez, M.; Boyd, A.; van Genuchten, M. Th.; Borghi, L.; Couto, P. and Raoof, A. (2020). Petrophysical correlations for the permeability of coquinas (carbonate rocks). Transport in Porous Media, 135, 287–308. https://doi.org/10.1007/s11242-020-01474-1

[51] Lima da Silva, D.; Ribeiro, A.; Terra, S.; and Borghi, L. (2024). A Three Stage Tectono-Stratigraphic Evolution of a Pre-Salt Rift Unit: Barra Velha Formation (Aptian) in the Tupi Field, Santos Basin, Brazil. SSRN. https://doi.org/10.2139/ssrn.4706897

[52] Macedo, J. (1989). Evolução tectônica da Bacia de Santos e áreas continentais adjacentes. Boletim de Geociências da Petrobras – Brasil, 3(3), 159–173.

[53] Mahjour, S.; Correia, M.; Santos, A. and Schiozer, D. (2019). Developing a workflow to represent fractured carbonate reservoirs for simulation models under uncertainties based on flow unit concept. Oil and Gas Science and Technology – Revue d'IFP Energies nouvelles, 74(2), 15. https://doi.org/10.2516/ogst/2018096

[54] Manifold, L.; El-Bozie, A.; Hollis, C. and Schröder, S. (2019). Characterizing facies, pore types, and diagenesis of a subtidal to peritidal carbonate platform for defining flow units. In: Carbonate Pore Systems: New Developments and Case Studies. SEPM Special Publication No. 112. https://doi.org/10.2110/sepmsp.112.03

[55] Mann, J. and Rigg, J. (2012). New geological insights into the Santos Basin. GeoExpro, 9(1), 36–40.

[56] Marghani, M.; Zairi, M. and Radwan, A. (2022). Facies analysis, diagenesis, and petrophysical controls on the reservoir quality of the low porosity fluvial sandstone of the Nubian formation, east Sirt Basin, Libya: Insights into the role of fractures in fluid migration, fluid flow, and enhancing the permeability of low porous reservoirs. Marine and Petroleum Geology, 147(11), 105986. https://doi.org/10.1016/j.marpetgeo.2022.105986

[57] Matonti, C.; Bourget, J.; Fournier, F.; Håkansson, E.; Pellerin, M.; Hong, F. and Reijmer, J. (2021). Distinct petroacoustic signature in heterozoan and photozoan carbonates resulting from combined depositional and diagenetic processes. Marine and Petroleum Geology, 128, 104974. https://doi.org/10.1016/j.marpetgeo.2021.104974

[58] Mattos, N.; Rebelo, T.; Leite, E.; Cataldo, R. and Batezelli, A. (2022). Quantitative seismic interpretation of the Barra Velha Formation in the Santos Basin, SE Brazil. SSRN Preprint, 38 p. https://doi.org/10.2139/ssrn.4237410

[59] Mehrabi, H.; Ataei, R.; Tavakoli, V. and Talebi, E. (2025). A quantification of the depositional–diagenetic heterogeneities in paleokarst hydrocarbon reservoirs: Sarvak Formation, Zagros Basin, Iran. Petroleum Research, In Press. https://doi.org/10.1016/j.ptlrs.2025.06.003

[60] Mello, V.; and Lupinacci, W. (2022). Mineralogy based classification of carbonate rocks using elastic parameters: A case study from Buzios Field. Journal of Petroleum Science and Engineering, 209, 109962. https://doi.org/10.1016/j.petrol.2021.109962

[61] Mendes, L. C.; Correia, U. M. C.; Cunha, O. R.; Oliveira, F. M.; and Vidal, A. C. (2022). Topological analysis of fault network in naturally fractured reservoirs: A case study from the pre-salt section of the Santos Basin, Brazil. Journal of Structural Geology, 159, 104597. https://doi.org/10.1016/j.jsg.2022.104597

[62] Menezes, M.; Dal'Bó, P.; Smith, J.; Mattos, N.; Ribeiro, C.; Arena, M.; Santos, H.; Pires, G.; Watahe, P. and Borghi, L. (2025). The influence of diagenetic conditions and fault zones on karstification development in the Barra Velha Formation (Aptian of Santos Basin, Brazil). Marine and Petroleum Geology, 178, 107427. https://doi.org/10.1016/j.marpetgeo.2025.107427

[63] Minzoni, M.; Cantelli, A. and Thornton, J. (2019). Seismic-scale geometries and sequence-stratigraphic architecture of early Cretaceous syn-post rift lacustrine carbonate systems, pre-salt section, South Atlantic margins. In Sequence Stratigraphy: The Future Defined. https://doi.org/10.5724/gcs.17.193

[64] Mohriak, W. (2001). Salt tectonics, volcanic centers, fracture zones and their relationship with the origin and evolution of the South Atlantic Ocean: geophysical evidence in the Brazilian and West African margins. 7th International Congress of the Brazilian Geophysical Society, 1594–1597. https://doi.org/10.3997/2214-4609-pdb.217.374a

[65] Mohriak, W. (2003). Bacias sedimentares da margem continental brasileira. In: Geologia, Tectônica e Recursos Minerais do Brasil, 87, 165.

[66] Mohriak, W. (2012). Bacias de Santos, Campos e Espírito Santo. In: Geologia do Brasil. Beca Edições, São Paulo, 481–496.

[67] Mohriak, W.; Gordon, A. and Mello, M. (2021). Chapter 11: Origin and petroleum system of the Cabo Frio High between the Santos and Campos basins: reviewed integration of structural and paleogeographic reconstruction with the oil and gas systems. In: AAPG Memoir 124 – The Supergiant Lower Cretaceous Pre-Salt Petroleum Systems of the Santos Basin, Brazil, 273–324. https://doi.org/10.1306/13722323MSB.11.1853

[68] Mondal, I.; and Singh, K. (2024). Petrophysical insights into pore structure in complex carbonate reservoirs using NMR data. Petroleum Research, 9(3), 439–450. https://doi.org/10.1016/j.ptlrs.2024.03.004

[69] Moreira, J.; Madeira, C.; Gil, J. and Machado, M. (2007). Bacia de Santos. Boletim de Geociências da Petrobras – Brasil, 15(2), 531–549.

[70] Netto, P.; Pozo, M.; da Silva, M.; Gomes, M.; Mexias, A.; Ramnani, C. W.; Parizek-Silva, Y.; Borghi, L.; and Rios-Netto, A. (2022). Paleoenvironmental Implications of Authigenic Magnesian Clay Formation Sequences in the Barra Velha Formation (Santos Basin, Brazil). Minerals, 12(2), 200. https://doi.org/10.3390/min12020200

[71] Noreen, K., Azeem, T., Rehman, F., Amin, Y., Ahmad, Q.A., & Hussain, M. (2025). Analyzing the impact of clay minerals on the reservoir quality of the Lower Goru Formation using Unsupervised Machine Learning. DOI: 10.1371/journal.pone.0324793

[72] Oliveira, G.; Santos, M. and Roque, W. (2020). Constrained clustering approaches to identify hydraulic flow units in petroleum reservoirs. Journal of Petroleum Science and Engineering, 186, 106732. https://doi.org/10.1016/j.petrol.2019.106732

[73] Oliveira, L.; Pimentel, F.; Peiró, M.; Amaral, P.; and Christovam, J. (2018). A seismic reservoir characterization and porosity estimation workflow to support geological model update: pre-salt reservoir case study, Brazil. First Break, 36(9), 25–34.

[74] Peçanha, A.; Lupinacci, W.; Ferreira, D. and Freire, A. (2019). A workflow for reservoir characterization applied to presalt coquinas from the Linguado Field, Campos Basin, Brazil. Journal of Petroleum Science and Engineering, 183, 106451. https://doi.org/10.1016/j.petrol.2019.106451

[75] Penna, R. (2022). Seismic flow units discretization and petrophysical modelling [Master's thesis, Universidade Federal Fluminense]. Niterói, 126 p.

[76] Penna, R. and Lupinacci, W. (2020). Decameter-scale flow-unit classification in Brazilian presalt carbonates. SPE Reservoir Evaluation and Engineering, 23(4), 1420–1439. https://doi.org/10.2118/201235-PA

[77] Penna, R. and Lupinacci, W. (2021). 3D modelling of flow units and petrophysical properties in Brazilian presalt carbonate. Marine and Petroleum Geology, 124, 104829. https://doi.org/10.1016/j.marpetgeo.2020.104829

[78] Penna, R. and Lupinacci, W. (2024). Geostatistical seismic inversion and 3D modelling of metric flow units, porosity and permeability in Brazilian presalt reservoir. Petroleum Science, 21(3), 1699–1718. https://doi.org/10.1016/j.petsci.2024.02.013

[79] Pereira, A.; Nunes, R.; Azevedo, L.; Guerreiro, L. and Soares, A. (2017). Geostatistical seismic inversion for frontier exploration. Interpretation, 5(4), T477–T485. https://doi.org/10.1190/int-2016-0171.1

[80] Pereira, M. and Feijó, F. (1994). Bacia de Santos. In: Feijó, F. J. (Ed.), Boletim de Geociências da Petrobras – Estratigrafia das Bacias Sedimentares do Brasil: Bacia de Santos, Vol. 8, PETROBRAS, Rio de Janeiro, 283–296.

[81] Pereira, P.; Bordignon, F.; Azevedo, L.; Nunes, R. and Soares, A. (2018). Strategies for integrating uncertainty in iterative geostatistical seismic inversion. arXiv:1810.07405 [physics.geo-ph]. https://doi.org/10.48550/arXiv.1810.07405

[82] Petersohn, E. (2013). Bacia de Santos: Sumário geológico e área em oferta. Agência Nacional de Petróleo, Gás Natural e Biocombustíveis – Seminário Técnico, 34 p.

[83] Rashid, F.; Hussein, D.; Glover, P.W.J.; Lorinczi, P. and Lawrence, J.A. (2022). Quantitative diagenesis: Methods for studying the evolution of the physical properties of tight carbonate reservoir rocks. Marine and Petroleum Geology, 139, 105603. https://doi.org/10.1016/j.marpetgeo.2022.105603

[84] Rebelo, T.; Batezelli, A.; Mattos, N. and Leite, E. P. (2022). Flow units in complex carbonate reservoirs: A study case of the Brazilian pre-salt. Marine and Petroleum Geology, 140(4), 105639. https://doi.org/10.1016/j.marpetgeo.2022.105639

[85] Rojas, D. (2022). Modelo geomecânico dos reservatórios do Pré-Sal Brasileiro, Bacia de Santos, e sua relação com o regime de tensão, a potencial reativação de falhas e a orientação preferencial de trajetória de perfuração. Dissertação (Mestrado em Geociências) — Instituto de Geociências, Universidade Estadual de Campinas (UNICAMP).

[86] Rojas, D.; Batezelli, A. and Leite, E. (2023). Fault reactivation potential in a carbonate field in Brazil based on geomechanical analysis. Marine and Petroleum Geology, 150, 106131. https://doi.org/10.1016/j.marpetgeo.2023.106131

[87] Rosa, M.; Cavalcante, J.; Miyakawa, T. and Freitas, L. (2018). The giant Lula Field: World's largest oil production in ultra-deepwater under a fast-track development. Offshore Technology Conference. Paper OTC-29043. https://doi.org/10.4043/29043-MS

[88] Rush, J. and Rankey, E. C. (2017). Geostatistical facies modeling trends for oolitic tidal sand shoals. AAPG Bulletin, 101(8), 1341–1379. https://doi.org/10.1306/09221616032

[89] Saussus, D. and Sams, M. (2012). Facies as the key to using seismic inversion for modelling reservoir properties. First Break, 30(7). https://doi.org/10.3997/1365-2397.2012009

[90] Schrank, A.; Dos Santos, T.; Altenhofen, S.; Freitas, W.; Cembrani, E.; Haubert, T.; Dalla-Vecchia, F.; Barili, R.; Goulart Rodrigues, A.; Maraschin, A. and De Ros, L. (2024). Interactions between clays and carbonates in the Aptian Pre-Salt reservoirs of Santos Basin, Eastern Brazilian Margin. Minerals, 14(2), 191. https://doi.org/10.3390/min14020191

[91] Sharifi-Yazdi, M.; Rahimpour-Bonab, H.; Nazemi, M.; Tavakoli, V. and Gharechelou, S. (2020). Diagenetic impacts on hydraulic flow unit properties: insight from the Jurassic carbonate Upper Arab Formation in the Persian Gulf. Journal of Petroleum Exploration and Production Technology, 10, 1783–1802. https://doi.org/10.1007/s13202-020-00895-6

[92] Soares, A. (2001). Direct sequential simulation and cosimulation. Journal of the International Association for Mathematical Geology, 33(8), 911–926. https://doi.org/10.1023/A:1012246006212

[93] Soares, A.; Diet, J. and Guerreiro, L. (2007). Stochastic inversion with a global perturbation method. In: EAGE Conference on Petroleum Geostatistics. https://doi.org/10.3997/2214-4609.201403048

[94] Soares, M.; Bomfim, L.; Vidal, A.; Avansi, M..; Cunha, O.; Vásconez-García, R. and Medeiros, R. (2023). Presalt carbonate cyclicity and depositional environment: A combined BHI and NMR approach to Markovian cycles in the Barra Velha Formation (Santos Basin, Brazil). SSRN. https://doi.org/10.2139/ssrn.4403902

[95] Tadayoni, M.; Kialilbeyg, M. and Bin-Junin, R. (2020). A new approach to heterogeneity analysis in a highly complex carbonate reservoir by using borehole image and conventional log data. Journal of Petroleum Exploration and Production Technology, 10, 2613–2629. https://doi.org/10.1007/s13202-020-00930-4

[96] Terra, G.; Spadini, A.; França, A.; Sombra, C.; Zambonato, E.; Juschaks, L.; Arienti, L.; Erthal, M.; Blauth, M.; Franco, M.; Matsuda, N.; Carramal, N.; Moretti, P.; D'Avila, R.; Souza, R.; Tonietto, S.; Anjos, S.; Campinho, V. and Winter, W. (2010). Classificação de rochas carbonáticas aplicável às bacias sedimentares brasileiras. Boletim de Geociências da Petrobras, 18(1), 9–29.

[97] Terra, S.; Ribeiro, A.; Mafia, M.; Nepomuceno, F.; Silva, D. and Borghi, L. (2024). Deformational structures in the lower Barra Velha formation, Aptian, Atapu field, Santos Basin. Journal of South American Earth Sciences, 136, 104816. https://doi.org/10.1016/j.jsames.2024.104816

[98] Terra, S.; Silva, D.; Ribeiro, A.; and Borghi, L. (2023). The lower Barra Velha formation (Aptian) in the Atapu field, Santos basin: Geological model for a pre-salt succession. Journal of South American Earth Sciences, 131, 104589. https://doi.org/10.1016/j.jsames.2023.104589

[99] Tiab, D. and Donaldson, E. C. (2004). Petrophysics: Theory and Practice of Measuring Reservoir Rock and Fluid Transport Properties (4th ed.). Elsevier, Oxford, 894 p.

[100] Toledo, S.; Basso, M.; Chinelatto, G.; Mendes, L. and Vidal, A. (2022). Insights into the Morphology and Seismic Facies of the Barra Velha Formation, Santos Basin Brazil. Third EAGE Conference on Pre Salt Reservoirs, Nov 2022, Volume 2022, 1–5. https://doi.org/10.3997/2214-4609.202288038

[101] Tosca, N.; and Wright, V. (2018). Diagenetic pathways linked to labile Mg-clays in lacustrine carbonate reservoirs: a model for the origin of secondary porosity in the Cretaceous pre-salt Barra Velha Formation, offshore Brazil. In Reservoir Quality of Clastic and Carbonate Rocks (Vol. 435). Geological Society, London, Special Publications. https://doi.org/10.1144/SP435.1

[102] Vital, J.; Ade, M.; Morelatto, R. and Lupinacci, W. (2022). Compartmentalization and stratigraphic-structural trapping in pre-salt carbonate reservoirs of the Santos Basin: A case study in the Iara Complex. SSRN Preprint, 44 p. https://doi.org/10.2139/ssrn.428403

[103] Wood, H.; Barnett, A.; Follows, E.; Ribeiro, P.; Guha, J.; Wheeler, J.; and Avila, R. (2025). The importance of core for carbonate reservoir evaluation: a case study from the Barra Velha Formation, Santos Basin, Brazil. Geological Society, London, Special Publications. https://doi.org/10.1144/sp548-2023-159

[104] Wright, V. and Barnett, A. (2015). An abiotic model for the development of textures in some South Atlantic early Cretaceous lacustrine carbonates. Geological Society, London, Special Publications, 418(1). https://doi.org/10.1144/SP418.3

[105] Yang, M.; Tan, X.; Xu, F.; Hao, D.; Zhao, J.; Li, C.; Huang, J. and Li, P. (2025). Controlling factors and evolution of reservoirs in continental rift lacustrine carbonate factory: Insight from the Cretaceous ITP-BVE Formation in Brazil's Santos Basin. Frontiers in Earth Science, 13, 1551406. https://doi.org/10.3389/feart.2025.1551406

[106] Yarmohammadi, S.; KadKiodaie, A.; Rahimpour-Bonab, H. and Shirzadi, A. (2014). Seismic reservoir characterization of a deep water sandstone reservoir using hydraulic and electrical flow units: A case study from the Shah Deniz gas field, the South Caspian Sea. Journal of Petroleum Science and Engineering, 118, 21–33. https://doi.org/10.1016/j.petrol.2014.04.002

[107] Zalán, P.; Severino, M.; Oliveira, J.; Magnavita, L.; Mohriak, W.; Gontijo, R.; Viana, A. and Szatmari, P. (2009). Stretching and thinning of the upper lithosphere and continental-oceanic crustal transition in Southeastern Brazil. AAPG International Conference and Exhibition – Abstracts, 1 p.

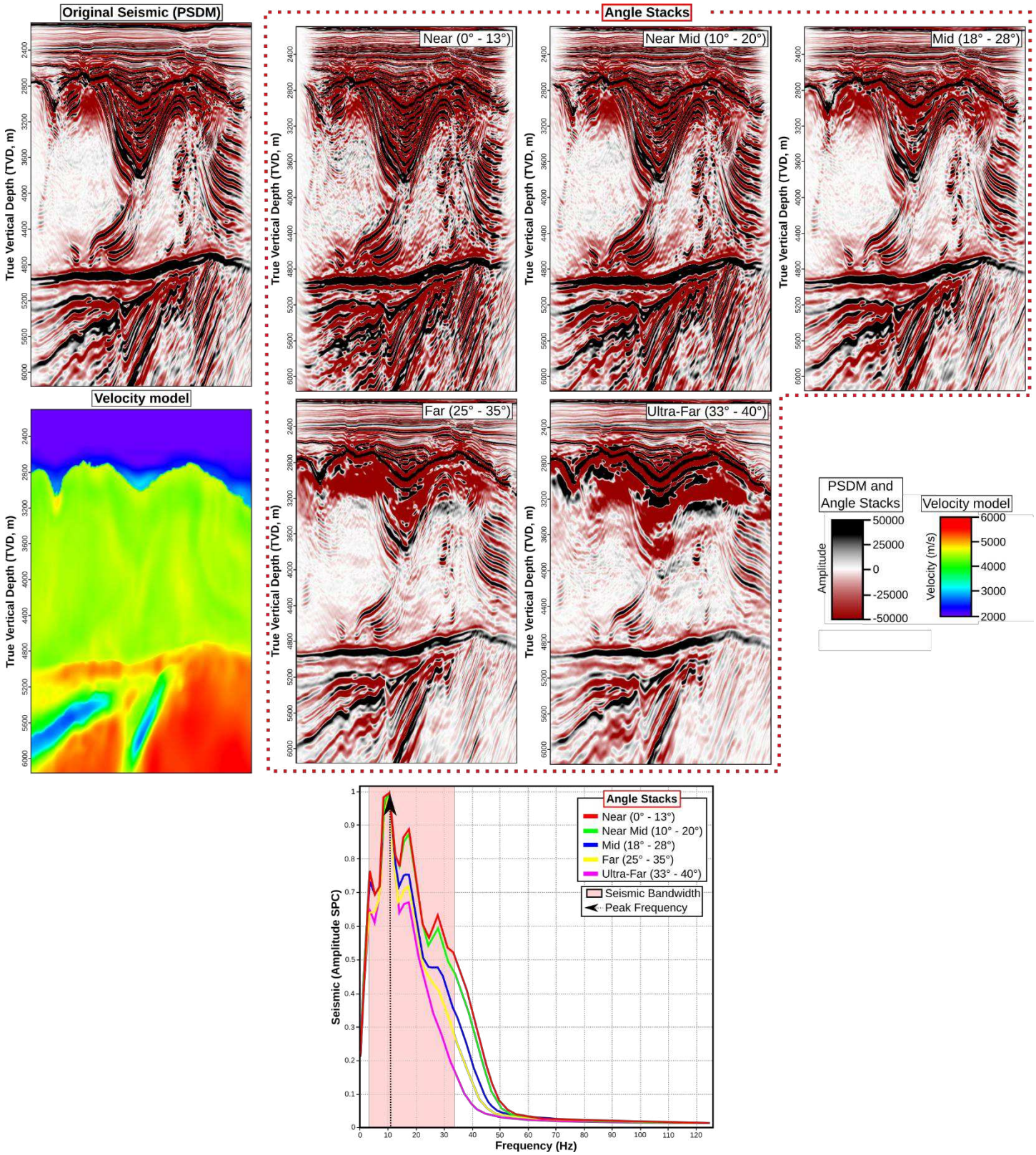


Fig. S1 – Upper: Seismic volumes on the study area: Original seismic – PSDM, angle-stacks (Near: 0°-13°, Near-Mid: 10°-20°, Mid: 18°-28°, Far: 25°-35° and Ultra-Far: 33°-40°) and velocity model. Lower: Amplitude spectrum of angle-stacks (Near, Near-Mid, Mid, Far and Ultra-Far), highlighting peak frequency (12 Hz) and useful bandwidth.

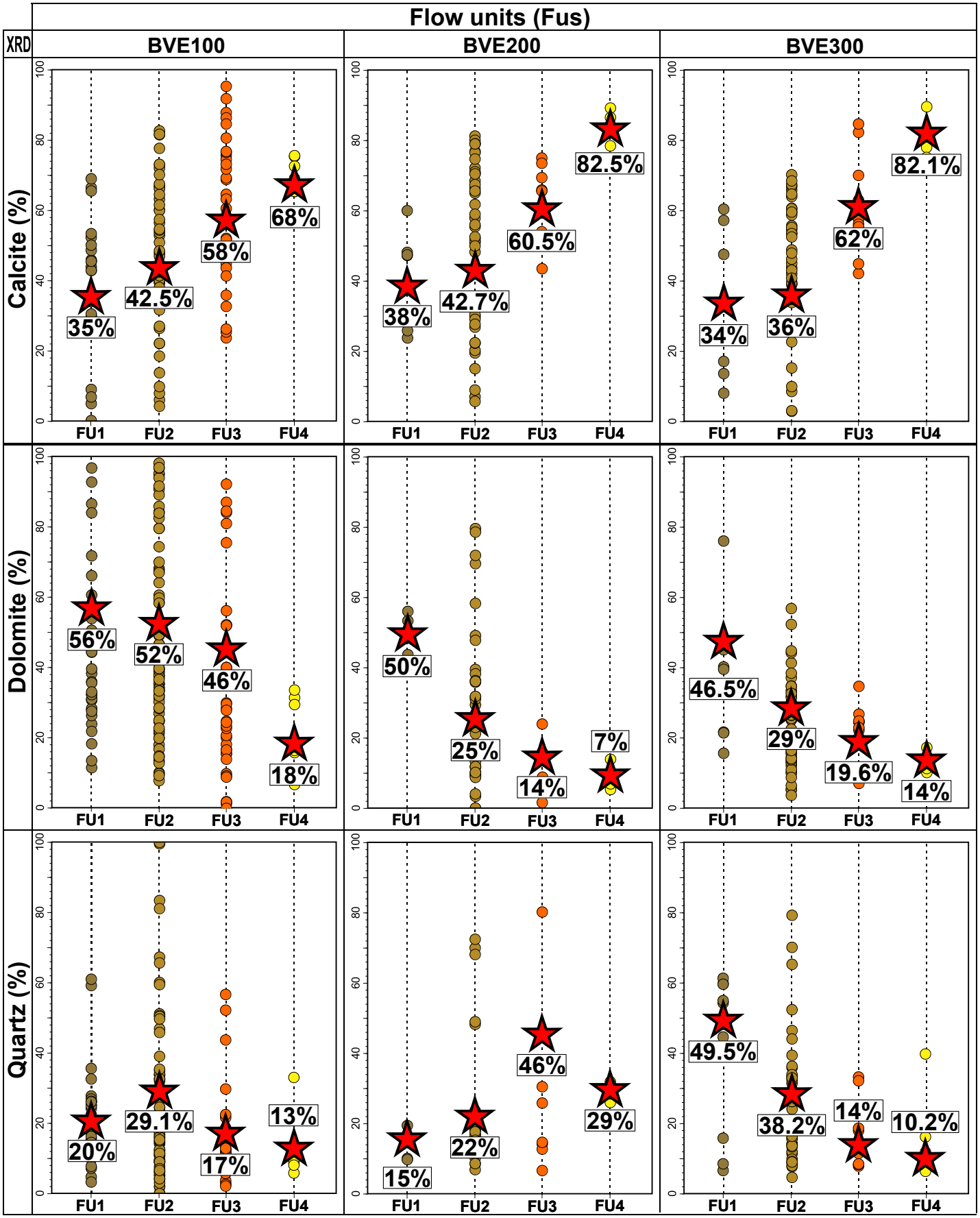


Fig. S2 – Mineralogical composition (calcite, dolomite and quartz) by FUs and production interval (BVE100, BVE200, and BVE300) of the Barra Velha Formation based on XRD analysis. The red star represents the average composition.

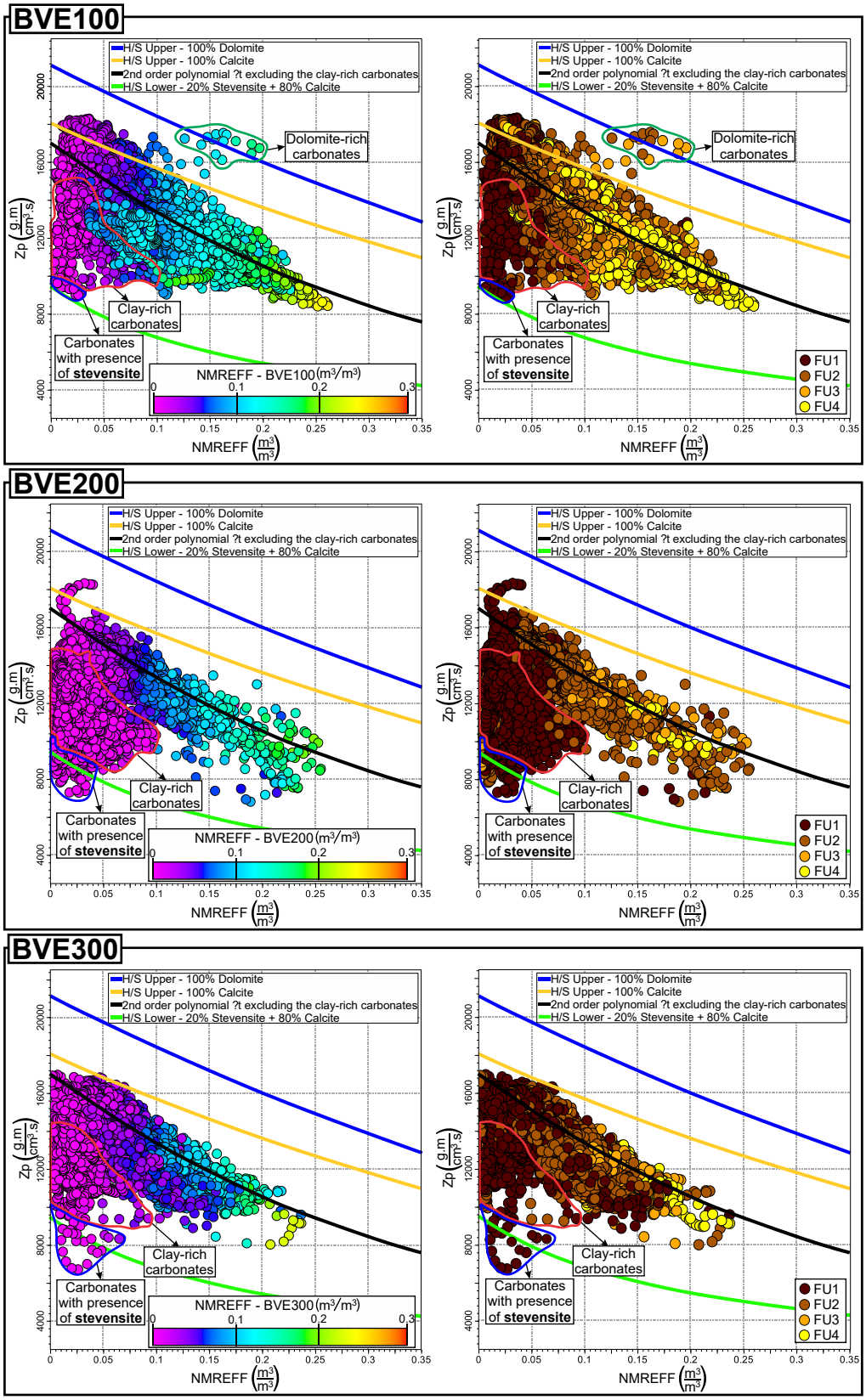


Fig. S3 – Relationship between Zp and NMREFF derived from well profiles for the producing intervals (BVE100, BVE200, and BVE300) of the Barra Velha Formation, highlighting the theoretical elastic limits of Hashin-Shtrikman (1963), the polynomial adjustment proposed by Mello and Lupinacci (2022), and the identification of dolomitic carbonates, rich in clay and with the presence of stevensite.

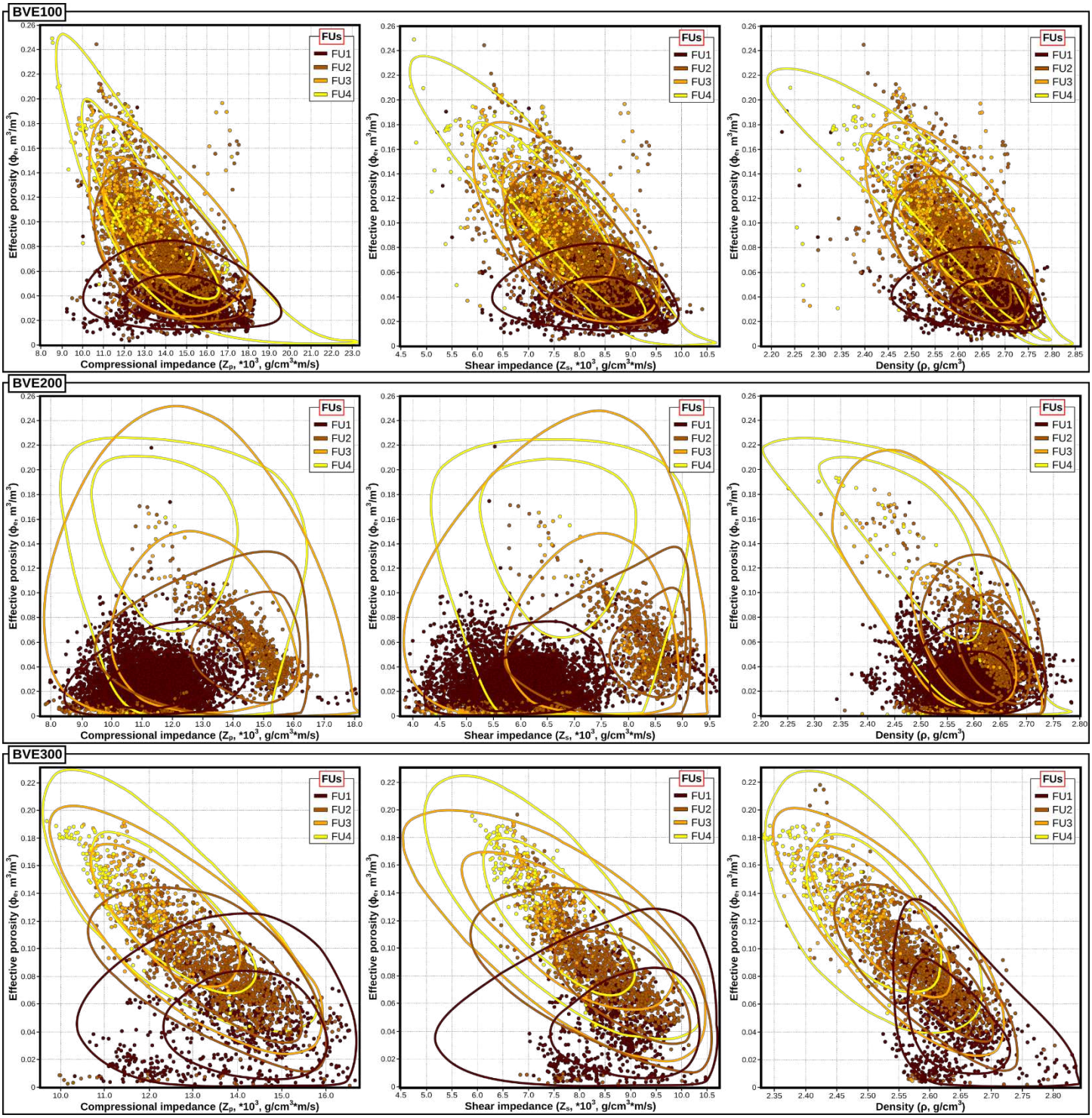


Fig. S4 – Bivariate joint distributions linking elastic properties (Zp, Zs, and density ρ) to effective porosity (ϕe) for the Barra Velha Formation, conditioned on hydraulic flow units (FUs). Ellipses indicate the main probability domains of the FUs.

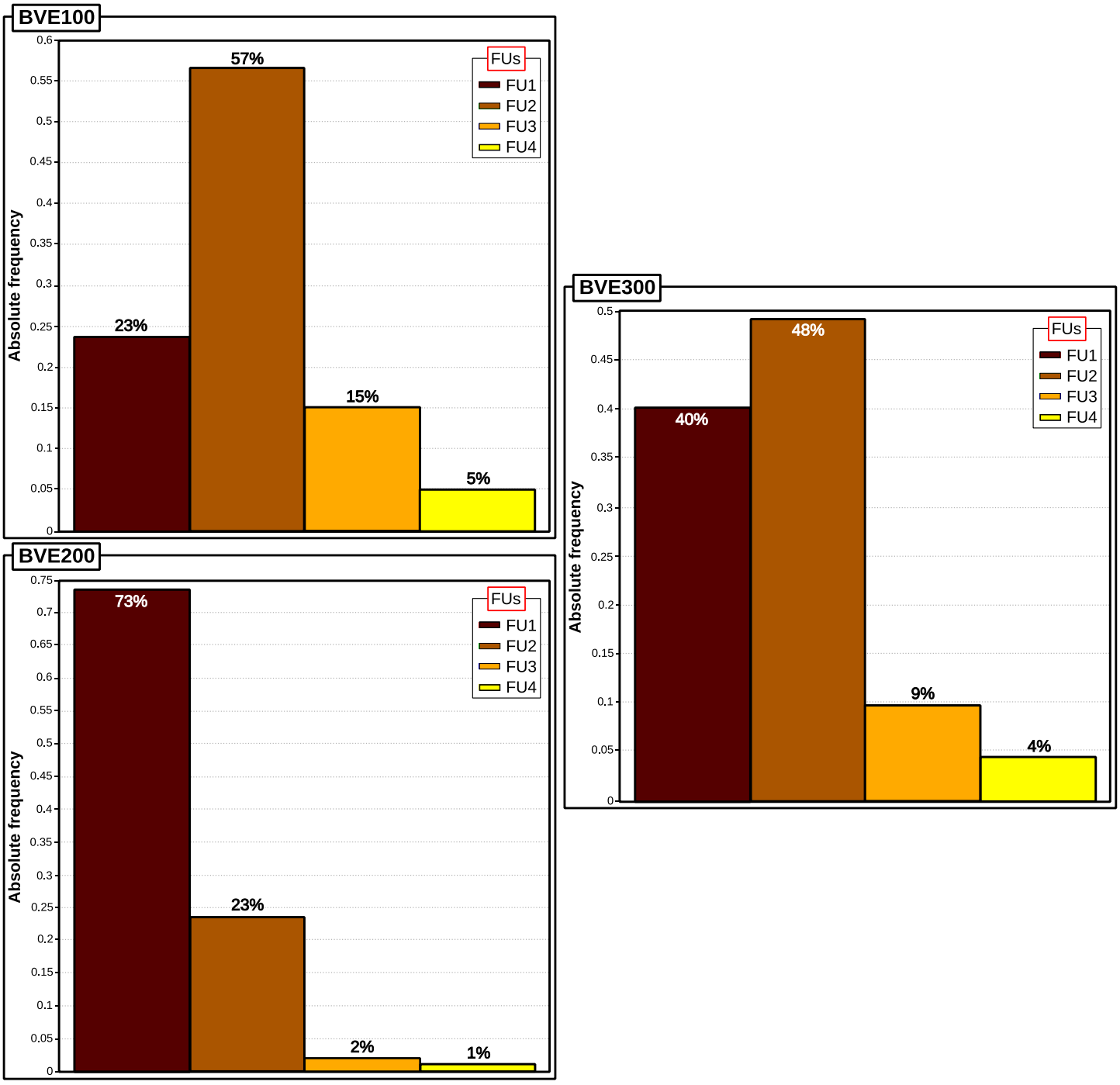
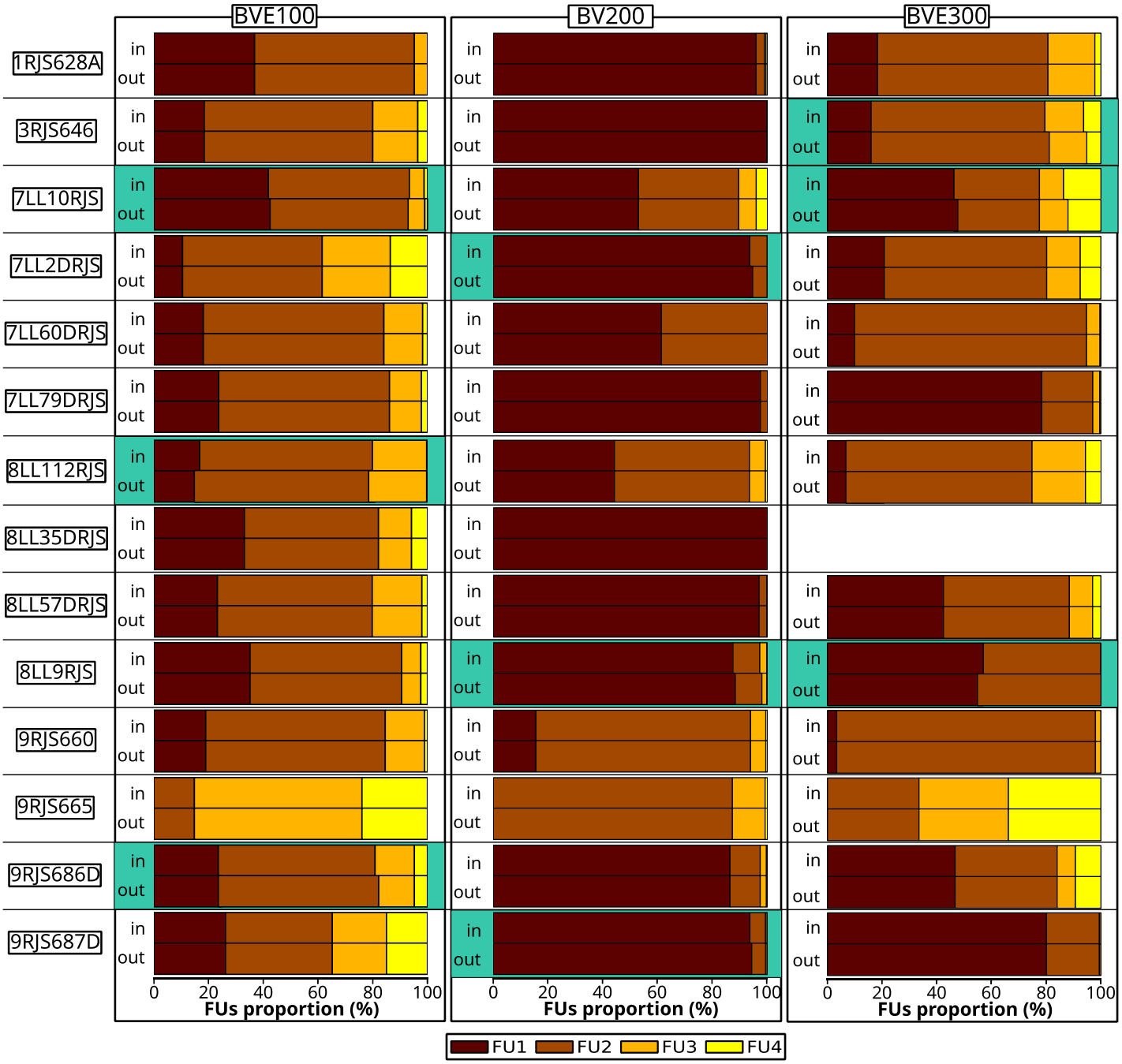


Fig. S5 – Proportional distribution of the hydraulic flow units (FU1–FU4) across the BVE100, BVE200, and BVE300 intervals of the Barra Velha Formation.



822

823 **Fig. S6 – Proportion of FUs by well before (input - in) and after (output - out) geostatistical seismic inversion, highlighting**
824 **control wells (constraints) in the BVE100, BVE200, and BVE300 production intervals.**